4.30 Thursday, Session 3 (afternoon): Godunov and ENO schemes

The generalised Riemann problem: the basis of ADER schemes

E. F. Toro* and V. A. Titarev

Department of Civil and Environmental Engineering, University of Trento, Mesiano di Povo, 38050 Trento, Italy

Advection-reaction type partial differential equations model a wide variety of phenomena in several disciplines in physics, chemistry, environmental sciences, geometry, financial mathematics and many others. Generally, these non-linear inhomogeneous equations must be solved in complicated multi-dimensional domains and thus analytical solutions are only available under very special circumstances. Situations in which exact solutions are available include Riemann problems. Conventionally, the Riemann problem for a system of conservation laws in two independent variables x and t is the initial value problem for the system with initial conditions consisting of two *constant* states separated by a discontinuity at the origin $x = 0$; for background see [3] and [8], for example. Ben-Artzi and Falcovitz [1] and others have generalised the concept of Riemann problem by admitting initial conditions that are *linear* functions in x, separated by a discontinuity at $x = 0$. We introduce the notation GRP_1 to denote this generalisation of the conventional Riemann problem, denoted by GRP_0.

Here we extend further the concept of generalised Riemann problem in two respects, the first concerns initial conditions and the second concerns the type of governing equations. As to initial conditions, we admit k-th order polynomial functions of x and denote the corresponding generalised Riemann problem by GRP_k. The most general case is that in which the initial conditions are two arbitrary but infinitely differentiable functions of x, with the corresponding generalised Riemann problem denoted by GRP_∞. Concerning the governing differential equations, in addition to pure non-linear advection, we include here reaction-like terms; these source terms are assumed to be arbitrary but sufficiently smooth algebraic functions of the unknowns.

We propose a semi-analytical method of solution of the generalised Riemann problem GRP_∞ for non-linear advection-reaction partial differential equations. The method gives the solution at $x = 0$ at a time τ, assumed to be sufficiently small, in terms of a time Taylor series expansion at $x = 0$ about $t = 0$. The leading term in this expansion is the exact solution of a conventional non-linear Riemann problem, GRP_0, with piece-wise constant initial conditions. All remaining terms in the expansion have coefficients that are time derivatives of the solution; these time derivatives are replaced by spatial derivatives by repeated use of the differential equations, a technique known as the Lax-Wendroff procedure [4]. It is then shown that all spatial derivatives in the expansion obey inhomogeneous advection equations. As derivative values are required at time $t = 0^+$, all source terms in these evolution equations for all-order spatial derivatives vanish and one only requires the solution of the conventional Riemann problems with piece-wise constant initial conditions for each of these advection equations. In summary, we reduce the solution of the generalised advection-reaction Riemann problem GRP_∞ to that of solving a sequence of conventional Riemann problems GRP_0 for homogeneous advection equations, the solutions of which are pieced together to determine the complete solution.

The approach can be extended further to solve the *general initial value problem* for advection-reaction partial differential equations with piece-wise smooth initial conditions for sufficiently small times. At any position x where the initial condition is smooth the GRP_∞ solution procedure applies trivially. In the case in which the initial condition includes more than one discontinuity, one places local origins at these positions to define local problems GRP_∞ and applies the solution method as described. In this manner, for a sufficiently short time, one obtains the solution everywhere at any point x that is sufficiently far away from points of initial discontinuities. This restriction is necessary to preserve time smoothness in the local Riemann problems. The solution technique presented here can be used for assessing the performance of numerical methods intended for solving complicated problems involving both non-linear advection and reaction. Given its local character, our solution procedure has also the potential for providing sub-cell resolution in numerical computation procedures for the general initial-boundary value problem. Finally, our solution procedure can be used to construct numerical methods of very high order of accuracy in space and time to solve the general initial-boundary value problem; results reported in [9], [11], [6], [7], [10], [5] look very promising. These methods extend existing numerical approaches such as those of Godunov [3] and Glimm [2] in which local solutions of conventional Riemann problems with piece-wise constant initial conditions are pieced together to advance the solution in time. Finally we make some remarks concerning the generalised Riemann problem for advection-diffusion equations.

References

[1] M. Ben-Artzi and J. Falcovitz. A Second Order Godunov–Type Scheme for Compressible Fluid Dynamics. *J. Comput. Phys.*, 55:1–32, 1984.

[2] J. Glimm. Solution in the Large for Nonlinear Hyperbolic Systems of Equations. *Comm. Pure. Appl. Math.*, 18:697–715, 1965.

[3] S. K. Godunov. Finite Difference Methods for the Computation of Discontinuous Solutions of the Equations of Fluid Dynamics. *Mat. Sb.*, 47:271–306, 1959.

[4] P. D. Lax and B. Wendroff. Systems of Conservation Laws. *Comm. Pure Appl. Math.*, 13:217–237, 1960.

[5] T. Schwartzkopff, C. D. Munz, E. F. Toro, and R. C. Millington. ADER-2D: A High-Order Approach for Linear Hyperbolic Systems in 2D. In *European Congress on Computational Methods in Applied Sciences and Engineering. ECCOMAS Computational Fluid Dynamics Conference 2001, Swansea, Wales, 4-7 September 2001*, pages –. -, 2001.

[6] V. A. Titarev. Very High Order ADER Schemes for Non-linear Conservation Laws. Masters Thesis by Research, Department of Computing and Mathematics, Manchester Metropolitan University, UK, 2001.

[7] V. A. Titarev and E. F. Toro. ADER: Arbitrary High Order Godunov Approach. *J. Scientific Computing, Special Issue (to appear)*, 2001.

[8] E. F. Toro. *Riemann Solvers and Numerical Methods for Fluid Dynamics, Second Edition*. Springer–Verlag, 1999.

[9] E. F. Toro, R. C. Millington, and L. A. M. Nejad. Towards Very High–Order Godunov Schemes. In *Godunov Methods: Theory and Applications. Edited Review, E. F. Toro (Editor)*, pages 905–937. Kluwer Academic/Plenum Publishers, 2001.

[10] E. F Toro and V. A. Titarev. ADER: Towards Arbitrary-Order Non-Oscillatory Schemes for Advection-Diffusion-Reaction. In *Proc. 8th National Conference on Computational Fluid Dynamics, E-Land, Taiwan, August 18-20, 2001*, pages 8–23, 2001.

[11] E. F Toro and V. A. Titarev. Very High-Order Godunov-Type Schemes for Non-linear Scalar Conservation Laws. In *European Congress on Computational Methods in Applied Sciences and Engineering. ECCOMAS Computational Fluid Dynamics Conference 2001, Swansea, Wales, 4-7 September 2001*, 2001.

High Order WENO Schemes for Hamilton-Jacobi Equations on Triangular Meshes

Yong-Tao Zhang* and Chi-Wang Shu

Brown University, USA

In this paper we construct high order weighted essentially non-oscillatory (WENO) schemes for solving the nonlinear Hamilton-Jacobi equations on two-dimensional unstructured meshes. The main ideas are nodal based approximations, the usage of monotone Hamiltonians as building blocks on unstructured meshes, nonlinear weights using smooth indicators of second and higher derivatives, and a strategy to choose diversified smaller stencils to make up the bigger stencil in the WENO procedure. Both third-order and fourth-order WENO schemes using combinations of second-order approximations with nonlinear weights are constructed. Extensive numerical experiments are performed to demonstrate the stability and accuracy of the methods. High-order accuracy in smooth regions, good resolution of derivative singularities, and convergence to viscosity solutions are observed.

On nonlinear amplification mechanism of instability near density discontinuities and shock waves for finite volume methods for Euler equations, place wave instability and carbuncle phenomena explanation

M. Abouziarov

Research Institute of Mechanics, Nizhni Novgorod State University

Despite constant progress in the development of numerical methods for Euler equations, some failings still remain [1]. The restriction, which follows from stability analysis of linearized equations, does not enough to provide the stability of some numerical schemes which are used to solve nonlinear problems with shock waves and big gradients. For these problems the intrinsic nonlinear behavior of equations is important [2, 3].
In this report the nonlinear analysis of stability of Euler equations for finite volume methods are presented. The substantial nonlinear amplification mechanism of numerical instability is demonstrated. It is is presented how the computer random errors are coupled with the nonlinear behavior of Euler equations and are amplified. It is established that the original Godunov's method is unstable.
¿From the obtained analytical results it is evident what is the reason of instability of plane wave in a wind tunnel and the origin of the "carbuncle phenomena".
¿From these analytical results it is rather obvious how to reconstruct numerical methods to avoid this nonlinear instability without changing the accuracy of the method, correcting only third order accuracy (dispersion) terms.
Numerical results demonstrating the efficiency of these corrections for the original Godunov's method and its second order modifications are presented.

References

[1] J. Quirk, "A contribution to the great Riemann solver debate," International Journal for numerical methods in fluids 18 (1994) pp. 555-574.

[2] M. Abouziarov, " Nonlinear stability analysis of Euler equations for predictor corrector schemes".GODUNOV'S METHOD FOR GAS DYNAMICS: Current Applications and Future Developments, A Symposium Honoring S.K. Godunov, May 1-2, 1997, The University of Michigan, Ann Arbor, Michigan

[3] M. Abouziarov, " On nonlinear stability analysis for finite volume schemes, plane wave instability and carbuncle phenomena explanation ". Second International Symposium on: "FINITE VOLUMES FOR COMPLEX APPLICATIONS - PROBLEMS AND PERSPECTIVES -" Duisburg, July 19-22, 1999, PP. 247-252.

Afternotes on PHM: Weighted Harmonic ENO methods

Antonio Marquina and Susana Serna *

University of Valencia, Spain

PHM methods have been used successfully as reconstruction procedure to design high-order Riemann solvers for nonlinear scalar and systems of conservation laws, (see [6], [1], [4]). We introduce a new class of polynomial reconstruction procedures based on the harmonic mean of the absolute values of the divided differences used as difference-limiter, following the original idea used before to design the piecewise hyperbolic method, introduced in [6]. We call those methods 'harmonic ENO methods', (HENO). Furthermore, we give analytical and numerical evidence of the good behavior of these methods used as reconstruction procedures for the numerical approximation by means of shock-capturing methods for scalar and systems of conservation laws in 1D and 2D in cartesian coordinates. We discuss, in particular, the behavior of a weighted fourth order harmonic ENO

method, (WHENO4 in short), compared with PHM, ENO and WENO methods, (see [2], [7], [3]), discussing the advantages and disadvantages.
Since the reconstruction procedures studied in this paper are scalar and one dimensional we will consider numerical approximations to weak solutions of the scalar conservation law:

$$u_t + f(u)_x = 0, \tag{1}$$

with the initial data, u_0, that is, a periodic or compactly supported piecewise smooth function:

$$u(x,t) = u_0(x), \tag{2}$$

We consider the following computational grid: $x_j = j\Delta x$, (Δx is the spatial step), $t_n = n\Delta t$, (Δt is the time step), $I_j = [x_{j-\frac{1}{2}}, x_{j+\frac{1}{2}}]$ is the spatial cell, where $x_{j+\frac{1}{2}} = x_j + \frac{\Delta x}{2}$ is the cell interface, $t_n = n\Delta t$, is the time discretization and $C_j^n = [x_{j-\frac{1}{2}}, x_{j+\frac{1}{2}}] \times [t_n, t_{n+1}]$ is the computational cell. Let u_j^n be an aproximation to the mean value in I_j, $\frac{1}{\Delta x}\int_{x_{j-\frac{1}{2}}}^{x_{j+\frac{1}{2}}} u(x,t_n)dx$, of the exact solution $u(x,t_n)$ of the initial value problem (1) and (2), obtained from a finite difference scheme in conservation form:

$$u_j^{n+1} = u_j^n - \frac{\Delta t}{\Delta x}(\tilde{f}_{j+\frac{1}{2}} - \tilde{f}_{j-\frac{1}{2}}), \tag{3}$$

where the numerical flux, $\tilde{f}$, is a function of $k+l$ variables

$$\tilde{f}_{j+\frac{1}{2}} = \tilde{f}(u_{j-k+1}, \cdots u_{j+l}), \tag{4}$$

which is consistent with the flux of the equation (1),

$$\tilde{f}(u, \cdots, u) = f(u). \tag{5}$$

For our purposes, a reconstruction procedure is an algorithm to obtain point values at the cell interfaces from cell averages and its differences corresponding to a set of discrete variables or fluxes, up to a degree of accuracy.
We want to reconstruct a function $g(x)$ from its mean values given at cells:

$$v_j = \frac{1}{\Delta x}\int_{x_{j-\frac{1}{2}}}^{x_{j+\frac{1}{2}}} g(x)dx \tag{6}$$

such that g is a piecewise smooth function associated to the spatial grid defined above, i.e., g restricted to each cell I_j is smooth, and, therefore, possible jump discontinuities are located at cell interfaces.
We will consider the following limiters, based on the harmonic mean between two nonnegative numbers:

$$\mathrm{harmod}(x,y) = (\mathrm{sign}(x) + \mathrm{sign}(y))\frac{|x||y|}{|x|+|y|}, \tag{7}$$

where $\mathrm{sign}(x)$ is the sign function, and

$$\mathrm{hareno}(x,y) = \mathrm{minsign}(x,y)\frac{2|x||y|}{|x|+|y|}, \tag{8}$$

where $\mathrm{minsign}(x,y) = \mathrm{sign}(x)$ if $|x| <= |y|$, and $\mathrm{minsign}(x,y) = \mathrm{sign}(y)$ otherwise. We recall that $\mathrm{minmod}(x,y)$ and $\mathrm{mineno}(x,y)$ are the well-known limiters, used respectively, for MUSCL and ENO methods, obtained by using the function $\min(|x|,|y|)$, instead of the harmonic mean in the above definitions.
There are many choices to design different polynomial reconstruction procedures by using harmonic limiters instead of ENO limiters. For instance, it is posible to get the harmonic MUSCL second order method by using the harmod limiter instead of the minmod one.
We focus our attention here on a fourth order accurate method, we call WHENO4, that uses the same stencil as the third order ENO, and it makes use either one harmonic averaged parabola or a weighted combination of two ones, chosen from five possible ones. In order to find the appropriate parabola(s) we apply the standard procedure of ENO3, for the first order differences, and, then, we use either the harmod or the hareno limiter between the nearest second order differences to the chosen first order difference to get a new second order difference. The resulting method is fourth order accurate in space and it behaves as a total

variation stable method when it is combined with the third-order Shu-Osher Runge-Kutta integration in time, (see [7]), under the standard CFL restriction.
The main advantage of this method compared with WENO5, (see [3]), is that does not use 'smooth indicators' to compute the weights, with the purpose to degenerate to digital ENO3 when discontinuities are present. WHENO4 does not degenerate to a third order accurate method, when discontinuities appear. The method is very low cost and simple to program and it behaves very accurate at local extrema. We will present several experiments to show the advantages and disadvantages of this method, compared with PHM, ENO3 and WENO5. As a sample, we show the behavior of this reconstruction at local extrema on the shock-entropy test, see figure 1, invented by Shu and Osher in ([7]).

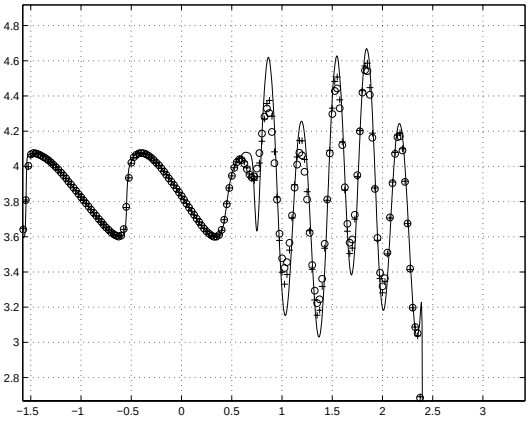

Figure 1: Shock entropy test: 400 points, time=1.8, CFL=0.1, 'Exact' solution vs. WHENO4, "o", WENO5, "+", zoomed region

References

[1] R. Donat and A. Marquina, *Capturing Shock Reflections: An improved Flux Formula* J. Comput. Phys., v. **125**, (1996) pp. 42-58.

[2] A. Harten, B. Engquist, S. Osher and S. Chakravarthy, *Uniformly High Order Accurate Essentially Non-oscillatory Schemes III*, J. Comput. Phys., v. 71, No. 2, (1987), pp. 231-303.

[3] G.S. Jiang and C. W. Shu, *Efficient Implementation of weighted ENO schemes,*, J. Comput. Phys., 126, (1996), p. 202.

[4] S. Li and L. Petzold, *Moving Mesh Methods with Upwinding Schemes for Time-Dependent PDEs*, J. Comput. Phys., v. 131, (1997), pp. 368-377.

[5] R.J. Leveque *Numerical methods for Conservation Laws*, Birkhauser Verlag, Zuerich, (1990).

[6] A. Marquina, *Local Piecewise Hyperbolic Reconstructions for Nonlinear Scalar Conservation Laws*, SIAM J. Sci. Comp., v. 15, (1994) pp. 892-915.

[7] C. W. Shu and S. J. Osher, *Efficient Implementation of Essentially Non-Oscillatory Shock Capturing Schemes II*, J. Comput. Phys., v. 83, (1989) pp. 32-78.

4.31 Thursday, Session 4 (morning): Central schemes II

Adaptive second order central schemes on unstructured staggered grids

Marc Küther and Mario Ohlberger*

Institut für Angewandte Mathematik, Universität Freiburg, Germany

This communication is devoted to the derivation and numerical implementation of adaptive central schemes on unstructured grids for approximating nonlinear hyperbolic conservation laws in several spatial dimensions.
First and second order central schemes on staggered grids were introduced by Nessyahu and Tadmor in 1990 [4] in one spatial dimension and generalized to particular unstructured grids in two space dimensions by Arminjon and Viallon in 1999 [1]. In [3] first order central schemes were generalized to arbitrary unstructured staggered grids. In addition, a posteriori error estimates were obtained, by interpreting the central scheme on staggered grids as a upwind finite volume scheme in conservation form on the intersection grid accompanied by suitable prolongation and restriction steps. Hence, the theory developed in [2] could be applied.
In this contribution we focus on the derivation of second order central schemes on a general class of unstructured grids in arbitrary spatial dimensions. The second order accuracy is achieved by using a reconstruction and limitation procedure. Furthermore we propose an adaption strategy for the first and second order methods where we use the theoretical a posteriori result of the first order scheme to derive appropriate refinement indicators.
We finally implemented this scheme in two spatial dimensions based on a primal triangular mesh for odd time steps and on a dual - Donald type - mesh for even time steps. Numerical experiments and comparisons with second order upwind methods demonstrate that the adaptive second order central scheme performs very well.

References

[1] P. Arminjon and M.-C. Viallon. Convergence of a finite volume extension of the Nessyahu-Tadmor scheme on unstructured grids for a two-dimensional linear hyperbolic equation. *SIAM J. Numer. Anal.*, 36:738–771, 1998.

[2] D. Kröner and M. Ohlberger. A-posteriori error estimates for upwind finite volume schemes for nonlinear conservation laws in multi dimensions. *Math. Comput.*, 69:25–39, 2000.

[3] M. Küther. Error estimates for the staggered Lax-Friedrichs scheme on unstructured grids. *SIAM J. Numer. Anal.*, 39(4):1269–1301, 2001.

[4] H. Nessyahu and E. Tadmor. Non-oscillatory central differencing for hyperbolic conservations laws. *J. Comput. Phys.*, 87:408–463, 1990.

New 2^{nd} Order Finite Volume Method Staggered in Space and Interleaved in Time

P. Arminjon*

Département de Mathématiques et de Statistiques, Université de Montréal, Canada

A. St-Cyr

CFD lab, Department of Mechanical Engineering, McGill University, Canada

A new modified version of the Nessyahu-Tadmor (NT) 1-dimensional finite volume central scheme is presented , as well as corresponding new versions for 2D-structured and 3D-unstructured grids inspired from the NT scheme. The modification avoids the intermediate predictor time step between t^n and t^{n+1}. Although this does not really lead to substantial accuracy /

computer time improvements in the 1D case, in the 2 and 3 dimensional cases, the modified scheme does lead to important reductions in computer times. 3D comparative simulations for a supersonic inviscid flow through a channel with a 4% bump are presented.

Efficient High-Order Central Schemes for Multi-dimensional Hamilton-Jacobi Equations

Steve Bryson*

Stanford University/NASA Ames Research Center, USA

Doron Levy

Stanford University, USA

We present new numerical schemes for approximating solutions of multi-dimensional Hamilton-Jacobi (HJ) equations of the form

$$\frac{\partial}{\partial t}\phi(x,t) + H\left(\frac{\partial}{\partial x}\phi(x,t), x\right) = 0, \qquad x \in R^N.$$

We develop non-staggered first- and second-order non-oscillatory central methods in any space dimension N. The locations of the evolution points for these schemes are carefully chosen to obtain an optimal time step. A great deal of efficiency is obtained by utilizing a projection step which recovers the solution at the original grid points. This projection step is one-dimensional, independently of the spatial dimensionality of the problem. Hence the computational requirements of these methods scale well with an increasing dimension N. This is important for HJ problems that arise, e.g., in control theory.
We also present third- and fifth-order Central Weighted Essentially Non-Oscillatory (CWENO) schemes for one-dimensional problems. These are the first high-order (order > 2) central methods for the HJ equations. Issues such as negative WENO weights that arise in the fifth-order case and optimization via the reuse of oscillatory measures and the natural continuous extension of the Runge-Kutta method will be discussed in detail. Efficient extensions of these high-order schemes to any space dimension N will be discussed.

4.32 Thursday, Session 4 (afternoon): Adaptive methods III

High-Order Single-Step Methods for Hyperbolic Initial-Boundary Value Problems

Thomas Hagstrom

The University of New Mexico, USA

In this talk we outline our work on the development of new methods for computing smooth solutions on structured meshes to hyperbolic initial-boundary value problems. Our goal is to enable the stable and efficient application of very high order difference methods in complex geometry. Primary barriers to be overcome include instabilities associated with one-sided differencing near boundaries, small cells near boundaries for Cartesian meshes, and storage and stability costs of high-order time-marching methods from the Runge-Kutta or Adams families.

Stabilization of one-sided differencing:

As is well-known, one-sided differencing on a uniform mesh is unstable. To date, the best methods for overcoming this problem combine approximations to d/dx which satisfy summation-by-parts rules with penalty formulations. Although theoretically available at all orders, their practical use has been limited, to our knowledge, to sixth order.

We are pursuing a different, inherently simpler approach - the stabilization of standard one-sided differencing by simple modification of a uniform grid near the boundary. The basic underpinning of this work is the belief that the root cause of the instabilities is the Runge phenomenon, not downwinding. Thus we simply insert one or two extra grid planes near the boundaries and move a few others. To illustrate the dramatic effect, consider first the twelfth order approximation to d/dx on an interval of length one with $u = 0$ at the right boundary and a uniform mesh of width h. Computing the eigenvalues of the differentiation matrix, an explosive instability is evident as an eigenvalue exists with:

$$\Re\lambda \approx 0.8 \cdot h^{-1}.$$

Now consider the effect of inserting two extra points located at distances $.1h$, $.5h$ from each boundary and displacing the first and last interior node on the uniform mesh from a distance of h to a distance of $1.2h$ from the boundary. The approximation is then stabilized with all eigenvalues lying in the left half-plane. Moreover, the spectral radius satisfies:

$$\rho \approx 2.35 \cdot h^{-1}.$$

Thus stability limits for standard time-stepping schemes are comparable to those for a low order method on the uniform grid. (The spectral radius can be further decreased by optimizing the node location.)

Topics to be addressed include:

i. Systematic optimization of the number and location of the extra nodes;

ii. Proofs of stability based on modified GKS theory;

iii. Numerical experiments with variable coefficient problems and nonrectangular domains.

Single-step methods in time:

At this time, the method-of-lines strategy for time-stepping is the typical choice. This approach is limited by the capabilities of standard ordinary differential equation solvers. Adams methods suffer from severe stability constraints and storage requirements at high order. Classical Runge-Kutta methods require more storage and work per step, but have larger stability regions. Recently, low-storage Runge-Kutta methods have been introduced which allow stages to be overwritten, thus reducing memory demands. In any event, it seems that Runge-Kutta methods presently in use are limited to fourth or fifth order.

We are examining alternative single-step methods recently proposed by Goodrich. These employ staggered grids and have the following general description:

a. Choose the stencil width, $2m$, and, for Hermite versions of the method, the order, q, of spatial derivatives to be carried.

b. Construct a local degree $(2m(q+1)-1)^d$ tensor-product polynomial approximation to each field on each cell and advance it in time via a Taylor series of the same order, evaluating the result, along with necessary derivatives, at the cell center.

c. Repeat the process on the dual grid, producing solution updates on the original grid.

In contrast with the method-of-lines approach, these new methods have the following favorable properties:

- They require no additional storage;
- They deliver the same order of accuracy in time as in space; (Goodrich has to date implemented methods of order 15, but there is no theoretical limitation.)
- They are well-suited for parallelization as the high-accuracy in time allows large time steps to be taken and no communications are required within a given step;
- They are dissipative;
- They are stable under the standard CFL constraint, $c\Delta t \leq \Delta x$.

A complication with the single-step methods is the derivation of the recurrence relations for the Taylor series in time for the function and, in the Hermite case, for its derivatives. This requires repeated space-time differentiation of the governing equations and efforts to reuse as many terms as possible in order to maximize efficiency. However, for special systems with simple nonlinearities, such as the Euler equations, these difficulties are easily managed.
The order, $2m(q+1)-1$, can be increased either by carrying more derivatives (increasing q) or by widening the stencil (increasing m). At first glance, it might seem that stencil widening would always be preferable, as no new unknowns are introduced. However, this is compensated for by the fact that the error constants for methods with narrow stencils and more derivative data are much smaller than those for methods with wide stencils and less derivative data. Indeed, Hermite methods are capable of resolving multiple wavelengths per grid spacing. In three dimensions, methods using derivatives of order q require $O(q^3)$ additional variables at each point. However, methods of the same order which don't use derivative data require $O(q^3)$ more points and an $O(q^{-1})$ smaller time step, Thus for problems with sufficiently simple coefficients and boundary conditions, it is better to use more derivative data. Also, the narrow stencils greatly ease the task of stably imposing boundary conditions. If $m = 1$ we require no special one-sided formulas near boundaries.
In the talk we plan to:

i. Describe the connection between the method's dissipativity and the use of grid staggering;

ii. Illustrate its properties through simple numerical experiments;

iii. Analyze the optimal choice of m and q;

iv. Consider its combination with the special grids described above.

We also mention a related effort involving a novel approach to the discretization of the wave equation on Cartesian meshes in complex geometry. The basis of the method is a new integral evolution formula for the wave equation. The new formula allows the construction of high-order, two-step, explicit methods which are unconditionally stable. This is possible since the integral formulation automatically leads to full compliance with domain of dependence requirements. Thus the small cell problem associated with Cartesian meshes in complex geometry may be overcome. Although the formulas are quite specific to the wave equation, we believe they can be generalized to some special first order systems, specifically Maxwell's equations in piecewise homogeneous media, and combined with the discretization strategies discussed above.
We acknowledge the contributions of various colleagues to aspects of the work described above including John Goodrich of NASA Glenn Research Center, Jens Lorenz and Igor Nazarov of UNM, Jing Li and Leslie Greengard of the Courant Institute, and Brad Alpert of NIST-Boulder. Financial support was provided by NSF, NASA Glenn Research Center, and the Institute for Computational Mechanics in Propulsion (ICOMP).

An adaptive order Godunov type central scheme

Eitan Tadmor and Jared Tanner*

UCLA, USA

We present an adaptive order Godunov type central scheme for time dependent problems with piecewise smooth solutions. Godunov type schemes require edge detection and the recovery of pointvalues from cell averages. Traditionally edge detection is automatically achieved with non-linear limiters inherent in the polynomial pointvalue recovery. Our method uses Global edge detection which ensures no discontinuity crossings and consequently computational stability. Additionally, the global edge detection substantially reduces the computational cost. Pointvalues are then obtained with an adaptive order central scheme that incorporates the largest symmetric stencil possible without crossing discontinuities. Consequently, the spatial order of accuracy is proportional to the number of cells to the nearest discontinuity.

Moving Adaptive Meshes and Godunov's Scheme

Boris N. Azarenok* and Sergey A. Ivanenko

Computing Center of the Russian Academy of Sciences, Vavilov street 40, Moscow, GSP-1, 119991, Russia

It is well known that if the solution of flow equations has regions of high spatial activity, a standard fixed mesh technique is ineffective, since it should contain a very large number of mesh points. In case of hyperbolic problems of gas dynamics it is domains containing shock waves and contact discontinuities. A moving mesh adaptation algorithm is applied to reduce computational costs in practical modeling. In such an approach the grid nodes are relocated so that to increase mesh concentration in the domains of steep moving fronts, emerging steep layers, pulses and shock waves.

One of the adaptive mesh generation techniques is the variational approach based on the theory of harmonic mapping between surfaces and mesh cells convexity concept [1]. Approximation of the harmonic functional is executed in such a way that its discrete analogy has an infinite barrier on the boundary of the set of unfolded grids. The infinite barrier prevents the grid cells from degenerating that allows for generating unfolded grids both in any simply connected, including nonconvex, and multiply connected 2D domains. The barrier property is of particularly importance in the vicinity of shock waves where the cells are very narrow and maximal aspect ratio achieves 50 and larger [2]. When modeling 2D hyperbolic problems with discontinuous solution on the moving adaptive mesh it is possible to reduce the errors, caused by shocks smearing over the cells, by many factors of ten and therefore to increase significantly, by several times [2], the total error throughout the flow domain.

Such a mesh adaptation requires to use a flow solver updating the flow parameters at the new time level directly on the moving grid without interpolation from one mesh to another, since interpolation smears discontinuities that, in turn, causes the accuracy of modeling to reduce.

We present the Godunov Linear Flux Correction (GLFC) scheme, a finite-volume solver of the second order accuracy in time and space, to calculate the problems of ideal gas flow on the moving grids [2]. In this approach the 2D laws of conservation of mass, momentum and total energy are written in the integral form, or generalized formulation, as follows [4]

$$\oiint_{\partial V} \boldsymbol{\sigma} dxdy + \boldsymbol{a} dydt + \boldsymbol{b} dtdx = \mathbf{0} \tag{1}$$

Here x, y are space and t is time variables and we integrate over the boundary ∂V of an arbitrary control volume V in space $x-y-t$. The vector-valued values are

$$\boldsymbol{\sigma} = \begin{bmatrix} \rho \\ \rho u \\ \rho v \\ E \end{bmatrix}, \quad \boldsymbol{a} = \begin{bmatrix} \rho u \\ \rho u^2 + p \\ \rho uv \\ u(E+p) \end{bmatrix}, \quad \boldsymbol{b} = \begin{bmatrix} \rho v \\ \rho uv \\ \rho v^2 + p \\ v(E+p) \end{bmatrix},$$

where u, v, p, ρ are the velocity components, pressure and density. Total energy $E=\rho[e+0.5(u^2+v^2)]$, e is the specific internal energy. Equation of state is $p=(\gamma-1)\rho e$, where γ is the ratio of specific heats. The conservation laws (1) hold for any flow parameters both smooth and discontinuous and, therefore, these equations govern a real 2D gas flow.
We introduce a curvilinear moving grid in space $x-y-t$ and consider the hexahedral computing cell (or control volume), see Fig.1. The bottom face of the cell is taken at time level n and the top face at level $n+1$, four lateral faces generally form ruled surfaces rather than simple planes.

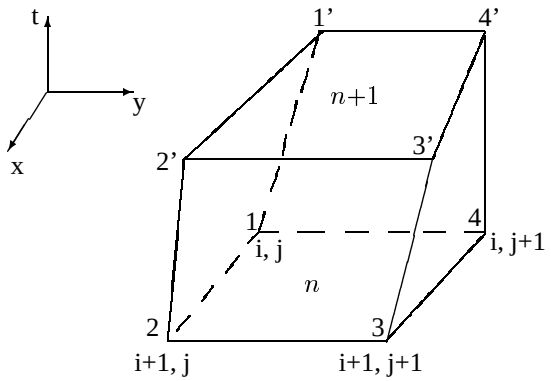

Fig. 1. Computing cell of the moving mesh

Integrating the system (1) over the oriented surface, being the boundary ∂V of the computing cell, we obtain a cell-centered finite-volume discretization of the governing equations

$$\boldsymbol{\sigma}^{n+1}A^{n+1} - \boldsymbol{\sigma}^{n}A^{n} + \boldsymbol{Q}_{411'4'} + \boldsymbol{Q}_{233'2'} + \boldsymbol{Q}_{122'1'} + \boldsymbol{Q}_{344'3'} = \mathbf{0}, \tag{2}$$

where $\boldsymbol{\sigma}^{n+1}$ and $\boldsymbol{\sigma}^{n}$ are the average values at time t^{n+1} and t^n in the center of the top and bottom faces, A^{n+1} and A^n are the areas of these faces. Each of four vector values $\boldsymbol{Q}_{411'4'}$, $\boldsymbol{Q}_{233'2'}$, $\boldsymbol{Q}_{122'1'}$ and $\boldsymbol{Q}_{344'3'}$ is an average flux of mass, momentum and energy through the corresponding intercell surface in the direction of the outward normal vector. The flow parameters at the next time level $(u,v,p,\rho)^{n+1}$ are updated via (2) using piecewise linear interpolation of the functions, monotonicity algorithm, time splitting and solution of the Riemann problem.
Coupled algorithm of using the GLFC scheme and adaptive moving mesh has been offered in [5]. Examples of using the coupled algorithm to model the 2D inviscid gas flow over the NACA0012 airfoil are shown in Figs. 2 to 5.
For the transonic case with $M_\infty=0.85$ and angle of attack $\alpha=1^\circ$ Fig.2 presents the Mach number contours computed on the quasiuniform and adapted O-meshes 140×80. Fragment of the adapted mesh is shown in Fig.3. We see that shock waves, one (stronger) on the upper side of the airfoil and the other (weakear) on the low side, are captured by strongly condensed grid lines. Thickness of the shocks reduces by 40-50 times in comparison with calculation on the nonadapted mesh that provides with capturing the shocks very accurately and allows to eliminate the errors caused by shocks smearing.
Another test is a supersonic flow over the same airfoil with $M_\infty=1.3$ and $\alpha=0^\circ$. Figs.4,5 present the Mach number contours computed on the quasiuniform and adapted O-meshes 120×50 and fragment of the adapted grid. One can see a strong bow shock appears in front of the airfoil leading edge and two weak shocks emanate from the trailing edge. Using adaptation provides with very strong reducing the bow shock thickness and rather strong reducing the trailing edge shocks thickness that is demonstrated by the both Mach number contours in Fig.4b and adapted mesh in Fig.5.

References

[1] S.A. Ivanenko , Harmonic mappings, *Chapt. 8 in: Handbook of Grid Generation*, J.F. Thompson et al eds., CRC Press, Boca Raton, Fl, (1999).

[2] B.N. Azarenok, Variational barrier method of adaptive grid generation in hyperbolic problems of gas dynamics, *SIAM J. Num. Anal.*, to appear. (See also http://www.math.ntnu.no/conservation/2001/042.html)

[3] B.N. Azarenok, Realization of a second-order Godunov's scheme, *Comp. Meth. in Appl. Mech. and Engin.*, **189** (2000), pp. 1031–1052.

[4] S.K. Godunov (Ed.), et al., Numerical Solution of Multi-Dimensional Problems in Gas Dynamics, *Nauka press, Moscow*, (1976), (in Russian).

[5] B.N. Azarenok, S.A. Ivanenko, Application of moving adaptive grids for numerical solution of nonstationary problems in gas dynamics, *Int. J. for Numer. Meth. in Fluids*, to appear.
(See also http://www.math.ntnu.no/conservation/2001/043.html)

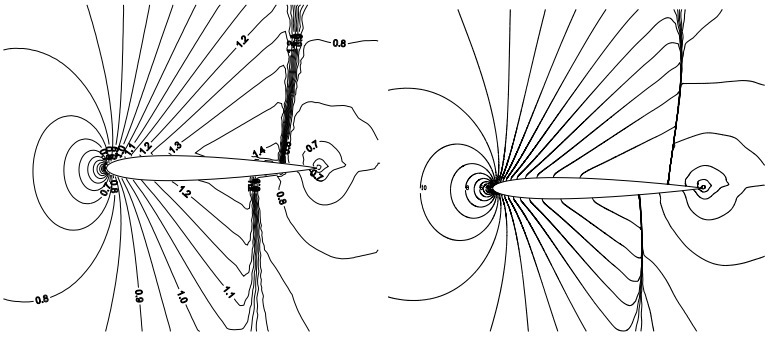

Fig. 2. Transonic flow around NACA0012 airfoil with M_∞=0.85 and angle of attack α=1°. Mach number contours computed on the quasiuniform (a) and adapted (b) meshs.

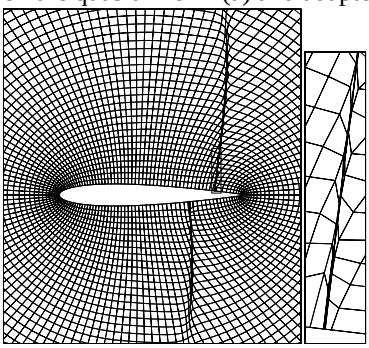

Fig. 3. Fragment of the O-mesh 140×80 around NACA0012 airfoil after adaptation for transonic flow calculations.

Adaptive Time Integration for Hyperbolic Conservation Equations

William J. Rider*, Len G. Margolin and James R. Kamm

Los Alamos National Laboratory, Los Alamos, NM 87545, USA

There have been two major approaches to improving time accuracy in numerical methods for hyperbolic conservation laws: the Lax-Wendroff [2] approach, and the method-of-lines [5]. Both of these are "linear" schemes in the sense that the same time differencing method is applied everywhere in the computational domain, usually for each timestep [1]. We distinguish these from "nonlinear" schemes, implying that the differencing depends on the local flow variables. In this sense, any nonlinear character in standard approaches to time differencing arises from the spatial differencing.
Nonlinear differencing in space has become the standard during the last twenty years, and is generally considered to be essential in effectively solving a broad range of applications. In this research, we explore the utility of nonlinear differencing in time, distinct from that used in space. We describe a methodology that allows the time and space differencing to adapt independently,

[1] Runge-Kutta methods are nonlinear in terms of Δt, that is their effective errors are nonlinear in terms of the step size, but linear in the sense that the method is not adapted to the nature of the local solution.

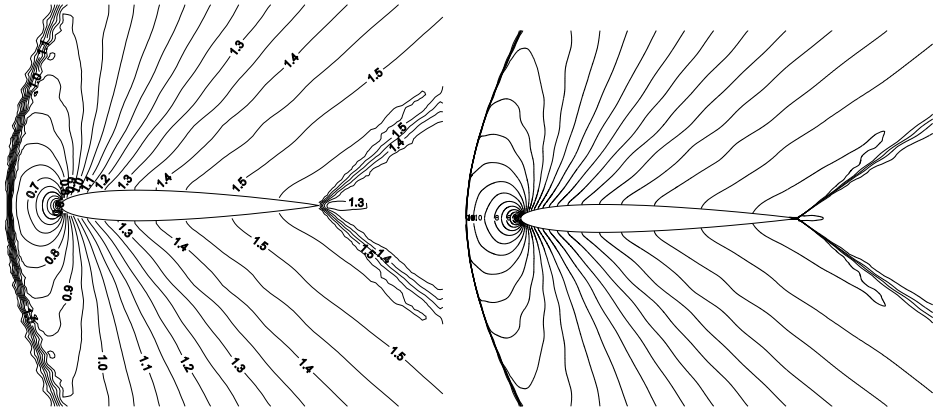

Fig. 4. Supersonic flow around NACA0012 airfoil with M_∞=1.3 and α=0°. Mach number contours computed on the quasiuniform (a) and adapted (b) meshs.

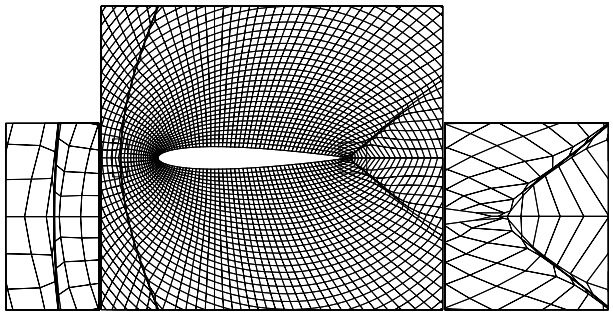

Fig. 5. Fragment of the O-mesh 120×50 around NACA0012 airfoil after adaptation for supersonic flow calculations.

and locally rather than globally. Finally, we examine the performance of this approach and show a situation where this method appears to yield greatly improved results.

We note that robust software for ordinary differential equations often adjusts the order of the integration scheme based on the local characteristics of the solution [1]. However, in that case the selected order of integration is typically applied to the entire system of ODEs. Extending this approach to a method-of-lines for hyperbolic conservation laws leads to a differencing that is global in space and time with temporal adaptivity, i.e., the same differencing is applied globally in space during a timestep, but varies from one timestep to the next. For example, the order is typically lowered when the estimates of the ordered expansion coefficients do not form a convergent sequence. On the other hand, if the coefficients indicate that the solution is smooth, the order might be increased. Such an approach would forfeit the advantages of modern shock capturing methods, where the order of integration is also spatially dependent upon the local (spatial) character of the solution. In particular, a shock wave is a local phenomenon whose presence should not necessitate the degradation of accuracy in smoother areas of the flow.

Lax-Wendroff techniques implicitly invoke the assumption of space-time similarity. It is assumed that the spatial truncation error will dominate the higher order temporal errors, guaranteeing a dissipative approximation and hence computational stability. While this situation may hold in many circumstances where the phenomena are (approximately) self-similar, it is not general. In particular, near a critical point, where the characteristic speed is nearly zero, the dissipation may vanish, thereby allowing higher-order terms to dominate. In our time adaptive methods, we define new "limiters" that depend on the time derivatives in a manner similar to the manner in which spatial limiters depend on spatial derivatives. In particular, we employ a nonlinear combination of time-differencing methods in the same manner that "upwind" and "downwind" differences are used to achieve

a desired property such as monotonicity or positivity preservation [2].
Our recent experience has shown that some difficulties may arise from other issues besides the breakdown of space-time similarity. Numerical algorithms can be viewed as dynamical systems [6]. One must be careful, therefore when implementing a time-differencing scheme, not to introduce spurious fixed points, which would be problematic for a wide variety of applications, including both steady and dynamic problems. Error control, upon which we base our adaptive time algorithms, has been shown to be an effective manner of combating spurious fixed points in solutions.
In designing our new methodology, we require that each cell edge allow an independent temporal integrator so that the resulting methods remain in conservation form. Thus, in one dimension we choose

$$u_j^{n+1} = u_j^n - \lambda \left[f(u)_{j+\frac{1}{2}} - f(u)_{j-\frac{1}{2}} \right], \tag{3}$$

where $f(u)_{j+\frac{1}{2}}$ has an order of time accuracy that is independent of any other edges. Here, u is the discretized dependent variable and f is the associated flux. Subscripts indicate the cell index and superscripts indicate discretized time level. In general, our scheme will depend on the temporal behavior in the zones that determine the flux; e.g., in the simplest case, the limiter will be constructed from u_j and u_{j+1} and its temporal derivatives. Although the spatial limiters will be evaluated at time n, as in the Lax-Wendroff or Runge-Kutta type approaches, we will now need to save previous fluxes or time-derivatives in an Adams-Bashforth fashion.
We have constructed our method in a simple form where temporal differences are tested, through a limiter, in the same manner as spatial differences are used for a Lax-Wendroff-style scheme. The temporal limiter is defined as

$$\widetilde{u_t} = \text{minmod}\left[(u_t)^n, 2(u_t)^{n-1} \right], \text{ or } = \text{minmod}\left[2(u_t)^n, (u_t)^{n-1} \right], \tag{4}$$

where in the most straightforward implementation, $(u_t)^{n-1} = \left(u^n - u^{n-1}\right)/\Delta t$ and $(u_t)^n = -\left[(f(u))_x\right]^n$, as in the Lax-Wendroff approach to time differencing. This is a straightforward form, resulting from using the backwards and forward time derivatives in place of spatial differences in a standard minmod limiter. We note that the extra time differences could be used to raise the temporal accuracy to third order

$$\widetilde{u_t} = \text{minmod}\left[\frac{5}{3}(u_t)^n - \frac{2}{3}(u_t)^{n-1}, 2(u_t)^n, 2(u_t)^{n-1} \right]. \tag{5}$$

There are two distinct outputs resulting from this approach: the actual update of the solution from the previous time step, and the identification of the presence of a critical point (i.e., a sign change in the time derivative). We will examine two cases, using the model equation,

$$\frac{\partial u}{\partial t} + u\frac{\partial u}{\partial x} = f(x,t), \tag{6}$$

i.e., inviscid Burgers' equation with a source term. The first case is a quasi-steady condition, where $\frac{\partial u}{\partial t} \approx 0$ so that $u\frac{\partial u}{\partial x} \approx f(x,t)$. This balance must be maintained for the computations to be well-behaved [3] and achieve the proper steady state. The second, perhaps more interesting case is where $u\frac{\partial u}{\partial x} \approx 0$, implying the balance $\frac{\partial u}{\partial t} \approx f(x,t)$. This indicates the presence of a stagnation point. Here, the balance between the source term and time derivative must be preserved by the numerical method. The proper evolution of the flow through dynamic critical points is crucial to the overall accuracy of the solution.
Our initial example is a scalar wave equation where one expects self-similarity to hold. We require from the outset that our methods should perform well in this important cases. The results are shown in Figure 1. In this case the flow is completely self-similar and the new method does not adversely effect the results. In other words, the time-limiter does not turn on except for where the spatial limiting has been activated. We also will examine this method's performance on Burgers' equation.
For the Euler equations we will start in one dimension. Considering at Sod's shock tube, we again see that our new method does not adversely influence the results. This is displayed for the density and velocity fields in Figure 2. Positive aspects of the new method are slightly reduced post shock oscillations and better resolution of the head of the rarefaction. In general, our new approach does not lower the resolution of solutions where self-similarity holds.
Although we expect that multidimensional examples of Euler or Navier-Stokes flows may exhibit more complex behavior than the examples above, we believe it is a necessary prerequisite for our schemes to perform well in these more idealized situations. We conclude by presenting a case where our approach provides a significant improvement for a nontrivial problem. The experiment [4] is a complex example of the evolution of a multidimensional fluid instability. Our attempts to analyze this

[2] One must take care when reducing the order of the temporal differencing; when coupled with high-order spatial differencing, the potential for oscillatory behavior arises. Where this is an issue, we drop the spatial accuracy as necessary to maintain stability.

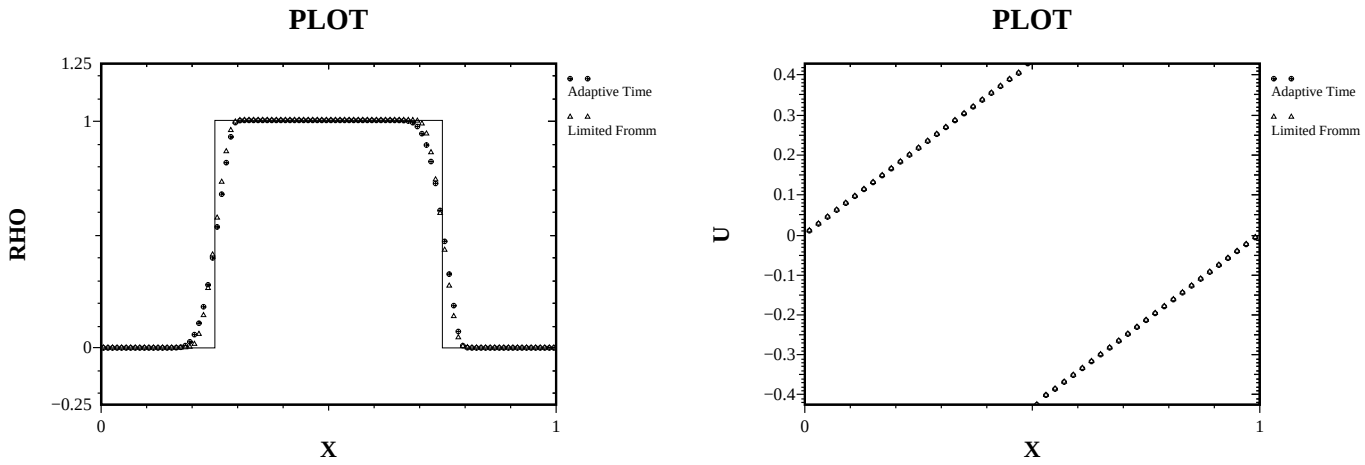

Figure 1: These two figures basically demonstrate that when self-similarity should hold that the time-limiter does not undermine the method's performance.

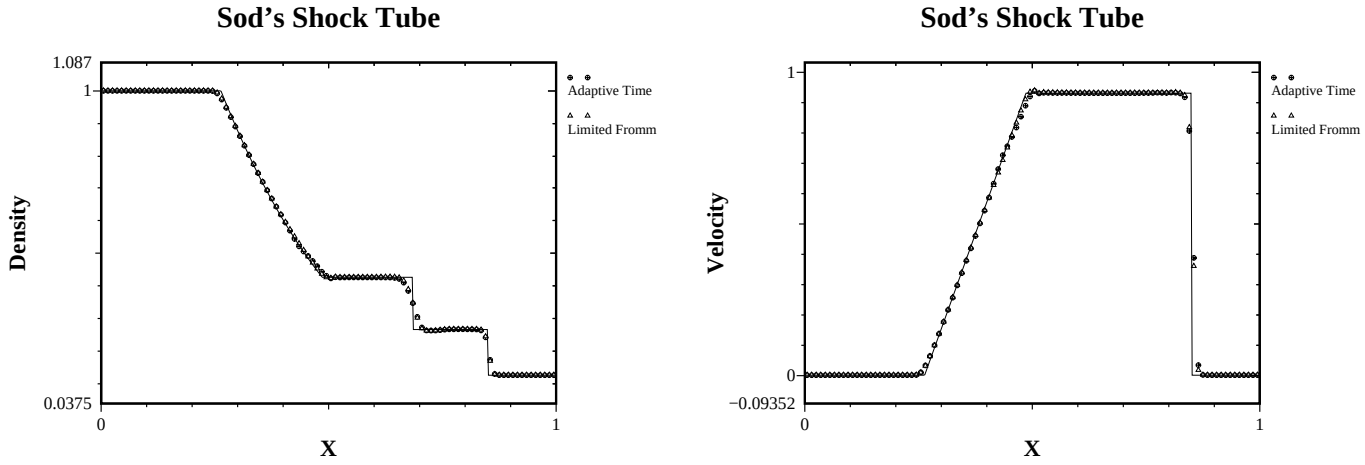

Figure 2: Results for Sod's shock tube are shown for a limited Fromm's scheme and a spatially limited Fromm's scheme with a time-limiter. The exact solution is given by the solid line.

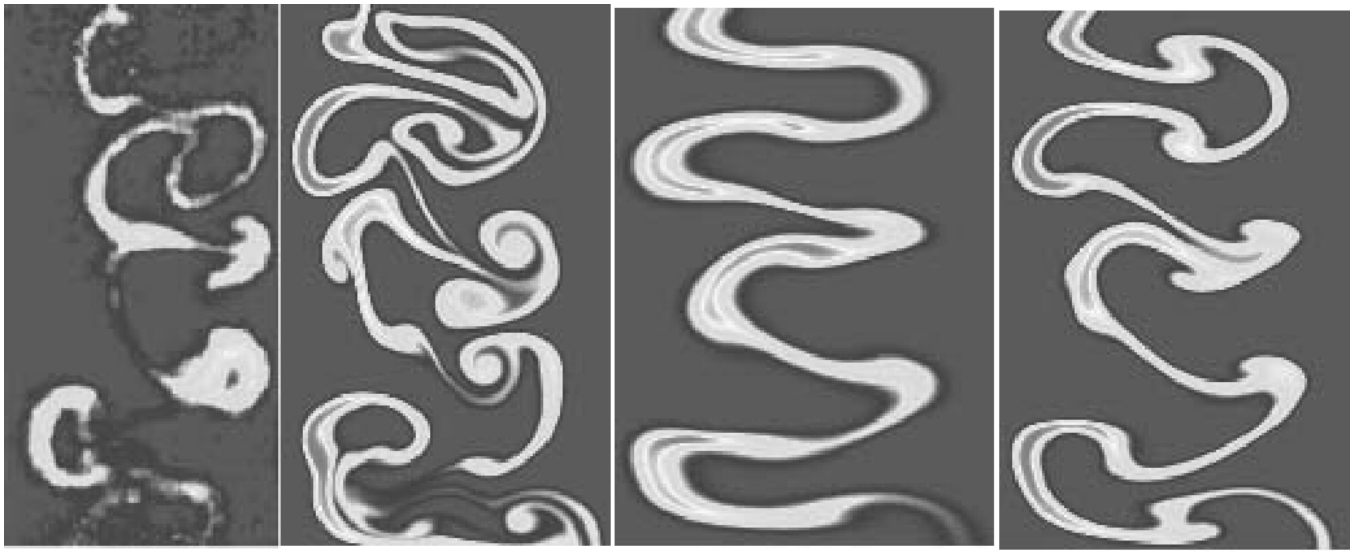

Figure 3: A montage of images from the gas curtain configuration showing the experimental data at 400 μs, and three simulations initialized from the experimental measurements. From left to right are the experimental images, a standard high-resolution Godunov method, a first-order Godunov method and a high-resolution Godunov method with time limiting. The visual differences in the simulations are striking.

experiment has provided both the initial impetus for our research as well as a framework to judge its utility. We have found that standard high resolution methods such as MUSCL, WENO, DG, TVD, etc., all produce solutions that are not consistent with the statistical behavior of the experimental data (as quantified by the fractal dimension, the wavelet spectra and the correlation-based measures of the density field). Of greater concern (and interest), we have found that a first-order Godunov method produces results more consistent with the observed statistical behavior. Further analysis of the simulations has localized the discrepancy to the behavior of the acoustic waves. We have found–and will document–that our adaptive time approach, as discussed above, leads to greatly improved results, in terms of their qualitative and quantitative agreement with the experimental data.
In summary, we have only begun to explore the possible formulations of time adaptivity. We believe that our preliminary results illustrate the power and flexibility of the approach, as well as its effectiveness. In particular, the ability to deal with problems that do not exhibit hyperbolic self-similarity should provide a new approach to attacking this difficult and important class of problems.

References

[1] U. M. Ascher and L. R. Petzold, *Computer Methods for Ordinary Differential Equations and Differential-Algebraic Equations*, SIAM, Philadelphia, PA, 1996.

[2] P. D. Lax and B. Wendroff, Systems of Conservation Laws, *Communications in Pure and Applied Mathematics*, **13**:217–237, 1960.

[3] L. G. Margolin and D. A. Jones, An Approximate Inertial Manifold for Computing Burgers' Equation, *Physica D*, **60**:175–184, 1992

[4] P. M. Rightley, P. Vorobieff, R. Martin & R. F. Benjamin, Experimental-observations of the mixing transition in a shock-accelerated gas curtain, *Phys. Fluids*, **11**:186–200, 1999.

[5] C.-W. Shu,Total-Variation-Diminishing Time Discretizations, *SIAM J. Sci. Comp.*, **9**:1073–1084, 1988.

[6] H. C. Yee, N. D. Sandham and M. J. Djomehri, On Spurious Behavior in CFD Simulations, *Int. J. Num. Meth. Fluids*, **30**: 675-711, 1999.

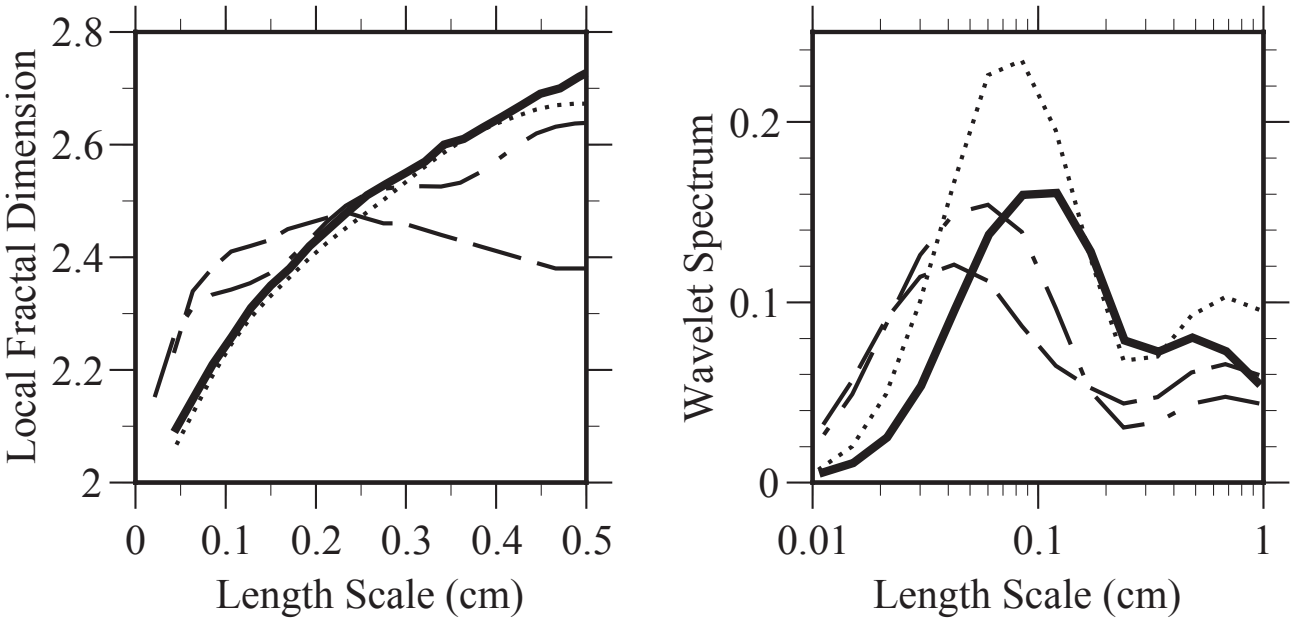

Figure 4: The statistical analysis of the images shown in Figure 3. The analysis uses fractals and wavelets to measure the properties of the images. The time-limited method is arguably the best match with the experimental statistics.

4.33 Thursday, Session 5 (morning): Viscosity and dissipation

Numerical Study of a Viscous Consolidation Model

Björn Sjögreen and Katarina Gustavsson *

Department of Numerical Analysis and Computer Science, Royal Institute of Technology, Sweden

Introduction

We consider the mathematical model

$$\phi_t + (v\phi)_y = 0 \quad (1)$$

$$\frac{4}{3}(\eta(\phi)v_y)_y - \frac{v}{D(\phi)} = p_s(\phi)_y + c\phi \quad (2)$$

describing a consolidation process of a flocculated suspension. A solid-fluid suspension is confined to a container of height H. Under the influence of gravity the suspension is separated into a solid and a liquid phase. The volume fraction of the particle phase is represented by $\phi = \phi(y,t)$ and the velocity by $v = v(y,t)$. The suspension is characterized by the viscosity, $\eta(\phi)$, the permeability, $D(\phi)$ and the yield pressure, $p_s(\phi)$. These functions are determined by experimental data and they are all non-negative functions of ϕ. The constant $c = G\Delta\rho$ where the gravity, G, is acting in negative y-direction and $\Delta\rho$ is the density difference between the phases. The problem is defined on the domain $[0, H]$ where boundary conditions for the velocity field, $v(0) = v(H) = 0$, and initial data for the volume fraction $\phi(y,0) = f(y)$ are specified.
We will show that the linearized problem is well-posed, present numerical methods approximating (1) and (2) and derive CFL stability conditions for these numerical methods.
The viscous term in equation (2) is of order $D(\phi)\eta(\phi)/H^2$ and is usually very small compared to the other terms. Therefore, it is more standard in consolidation modeling to solve the corresponding inviscid problem, obtained by setting $\eta(\phi) = 0$, see e.g. [1], [2] and [3] among others. In the inviscid model, we eliminate v from (1), and obtain

$$\phi_t - (c\phi^2 D(\phi))_y = (D(\phi)p_s(\phi)_y)_y \quad (3)$$

which we recognize as a hyperbolic conservation law with a viscous term. We will here show that the approximation of the inviscid problem has a considerably more restrictive CFL condition, than the viscous problem, thus making the viscous problem more suitable for a numerical solution. Another reason for treating the viscous problem is that it has features in common with the 2D consolidation model treated in [4]. Hence, the numerical methods developed here can easily be extended to the 2D consolidation model. For cases where both the viscous and inviscid models are applicable we show that they give similar results.

Well-posedness of the linearized problem

We first perform a simple analysis, by linearizing the equations (1) and (2) around a constant state, and by assuming a Cauchy-problem. We take the Fourier transform in space of the system, and let $\hat{v}(\xi,t)$ and $\hat{\phi}(\xi,t)$ denote the Fourier transformations of v and ϕ respectively. We eliminate $\hat{v}(\xi,t)$ from the transformed system, to obtain the equation $\hat{\phi}_t = \hat{P}(\xi)\hat{\phi}$ where the Fourier symbol is given by

$$\hat{P}(\xi) = i\xi(v_0 + \frac{D'(\phi_0)v_0\phi_0/D(\phi_0)^2 - c\phi_0}{4\eta(\phi_0)\xi^2/3 + 1/D(\phi_0)}) - \xi^2\frac{p_s'(\phi_0)\phi_0}{4\eta(\phi_0)\xi^2/3 + 1/D(\phi_0)}$$

From this symbol, we conclude that

- The equation is well-posed but not parabolic.
- The equation has features of both wave propagation and damping.
- The damping acts as viscosity in the low modes, and as a sink in the high modes.

Difference Approximation

We introduce grid points, $y_j = (j-1)\Delta y$, $j = 1, 2, \ldots, N$, on the interval $[0, H]$ where $\Delta y = H/(N-1)$. Let v_j denote the numerical approximation of $v(y_j)$. For the volume fraction, we use a staggered approximation, and define $\phi_{j+1/2}$, $j = 1, 2, \ldots, N-1$, the approximation of ϕ at the points $y_{j+1/2} = (y_j + y_{j+1})/2$. We will use the difference operators $D_+ u_j = (u_{j+1} - u_j)/\Delta y$ and $D_- u_j = (u_j - u_{j-1})/\Delta y$.
We approximate (1) and (2) by the semi-discrete difference approximation

$$\frac{d\phi_{j+1/2}}{dt} = -D_+ h_j \tag{4}$$

$$\frac{4}{3} D_+(\eta(\phi_{j-1/2}) D_- v_j) - \frac{v_j}{D(\bar{\phi}_j)} = D_+ p_s(\phi_{j-1/2}) + c\bar{\phi}_j \tag{5}$$

where $\bar{\phi}_j = (\phi_{j+1/2} + \phi_{j-1/2})/2$. The time integration can be done by a Runge-Kutta method, or by a linear multi step method. In the case of a second order central scheme, the numerical flux function, h_j, is

$$h_j = v_j \bar{\phi}_j. \tag{6}$$

This approximation is centered, and can perform badly in the neighborhood of steep gradients in ϕ. We therefore suggest using a TVD-like difference scheme on conservative form with

$$h_j = h(\phi_{j+1/2}, \phi_{j-1/2}) = v_j \bar{\phi}_j - \frac{\varepsilon}{2\lambda}(\phi_{j+1/2} - \phi_{j-1/2}) \tag{7}$$

where ε is a constant viscosity coefficient and $\lambda = \Delta t/\Delta y$. This flux function is improved to second order of accuracy by piecewise linear reconstruction,

$$h_j = h(\phi_{j+1/2} - s_{j+1/2}/2, \phi_{j-1/2} + s_{j-1/2}/2) \tag{8}$$

where the slopes, s, are obtained by the van Albada flux limiter.

Stability Analysis

We get a necessary condition for the stability of these difference approximations, by performing linear constant coefficient von Neumann analysis. This is done by applying the approximation (4) and (6) to the linearized problems. Under periodicity assumptions we transform to Fourier modes in space, in the standard way. Let $\hat{v}_\omega$ and $\hat{\phi}_\omega$ denote the Fourier coefficients. After elimination of $\hat{v}_\omega$, we obtain the equation $\frac{d\hat{\phi}_\omega}{dt} = \hat{Q}(\omega, \Delta y)\hat{\phi}_\omega$ with Fourier symbol

$$\begin{aligned} \hat{Q} &= -i\frac{\sin\omega\Delta y}{\Delta y}\left(v_0 - \frac{c\phi_0 - D'(\phi_0)\phi_0 v_0/D(\phi_0)^2}{16\eta(\phi_0)\sin^2(\omega\Delta y/2)/(3\Delta y^2) + 1/D(\phi_0)}\right) \\ &- \frac{4\sin^2(\omega\Delta y/2) p_s'(\phi_0)\phi_0/\Delta y^2}{16\eta_0 \sin^2(\omega\Delta y/2)/(3\Delta y^2) + 1/D(\phi_0)} \end{aligned}$$

If we use a time integration method which encloses a square $-a < \Re(z) < 0, -b < \Im(z) < b$ in its region of absolute stability, the CFL-conditions

$$\lambda(|v_0| + |c\phi_0 D(\phi_0) - D'(\phi_0)\phi_0 v_0/D(\phi_0)|) < b \qquad 3\Delta t p_s'(\phi_0)\phi_0/(4\eta(\phi_0)) < a \tag{9}$$

are sufficient to guarantee linear stability. The following facts are observed

- It is possible to assure stability, even if we let $p_s'(\phi)$ blow up like $1/\Delta t$ at some point.
- In the inviscid model with $\eta = 0$, the more restrictive condition $4p_s'(\phi_0)\phi_0 D(\phi_0)(\Delta t/\Delta y^2) < a$ is obtained. This shows that the viscous model has better numerical stability properties.
- The approximation analogous to (4) and (6), but on a non-staggered grid, will lead to a Fourier symbol having the factor $\sin^2(\omega\Delta y)$ instead of $\sin^2(\omega\Delta y/2)$ in the numerator of the real part of $\hat{Q}$, showing the problem with odd-even modes for this problem, in analogy with the incompressible Navier-Stokes equations.

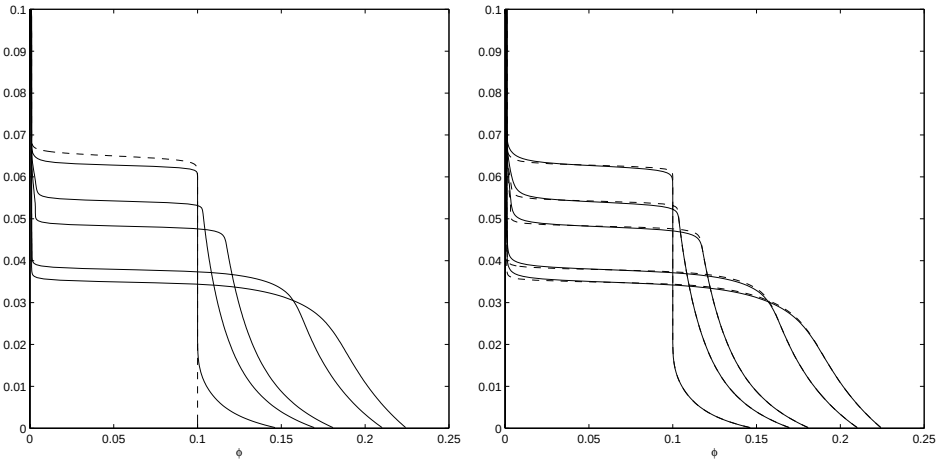

(a) ϕ at different times

(b) Comparison between viscous and inviscid model

Figure 1: Volume fraction, ϕ, as a function of y at different times, $t = 200, 1000, 2000, 10000$ and 20000 s. In the left figure the dashed line is the initial concentration. In the right figure we compare the solution obtained by the inviscid model (solid line) to the solution obtained by the viscous model (dashed line).

Numerical Experiments

From measurements, the following relations have been found correlating experimental data to the viscosity, permeability and yield pressure functions.

$$\begin{aligned} D(\phi) &= (1-\phi)k_D\phi^{n_D} \\ \eta(\phi) &= k_\eta\phi^{n_\eta} \\ p_s(\phi) &= \begin{cases} k_p\eta^{n_p} & \phi > \phi_g \\ 0 & \phi \le \phi_g \end{cases} \end{aligned}$$

The constants have been determined to the following values,

$$\begin{array}{lll} k_D = 4.6\times10^{-18} m^2\, Pa^{-1}\, s^{-1} & n_D = -7.41 & \\ k_\eta = 1.2691\times10^6 Pas & n_\eta = 3.4 & \\ k_p = 5\times10^6 Pa & n_p = 4.846 & \phi_g = 0.1 \end{array}$$

These functions have to be modified to make them more suitable for mathematical and numerical treatment. In light of the CFL stability limits (9) we require that the jump in the function $p_s(\phi)$ should be smoothed, so that the derivative $p_s'(\phi)$ is bounded. Furthermore, $\eta(\phi)$, should be prevented from going to zero as ϕ goes to zero. The viscosity should physically approach the viscosity of the liquid, when the particles disappear.
In the numerical experiments we used the initial data

$$\phi(y,0) = \phi_0(y) = (\phi_g - \phi_{min})\frac{1}{2}(1-\tanh(K(y-y_0))) + \phi_{min} \tag{10}$$

where $\phi_g = 0.1$, $\phi_{min} = 0.001$ and the regularizing parameter, $K = 1000$. The constant c takes the value $1.0\times10^6 kgm^{-2}s^{-2}$ in the computations.
A sequence of solutions to the viscous model, (1) and (2), at different times is shown in Fig. 1a. In Fig. 1b we show a comparison of solutions obtained by the viscous model and the inviscid model given by (3). The viscous term is small and the difference is small between the solutions. The computation with the viscous model required only around $1/50$ the CPU-time of the computation with the inviscid model. The advantage of the viscous model becomes even larger, when the grid is refined.

Table 1 shows a grid convergence study of the scheme given by (4), (5), (7) and (8) applied to the viscous model. The table shows second order accuracy. Here we use $K = 100$ in the initial data function to obtain a solution sufficiently smooth to measure the order of accuracy. The convergence exponent, p was estimated by the formula

$$p = \log\left(\frac{\|\boldsymbol{f}_{\Delta y} - \boldsymbol{f}_{\Delta y/3}\|}{\|\boldsymbol{f}_{\Delta y/3} - \boldsymbol{f}_{\Delta y/9}\|}\right) / \log 3 \tag{11}$$

where $\boldsymbol{f}$ is a vector valued function and $\|\cdot\|$ is either the discrete $L1$-norm, $L2$-norm or the $\max$-norm. The time step is chosen such that $\lambda = \Delta t/\Delta y$ is constant, where $\Delta t = 0.1$ on the coarsest mesh and $\Delta y = 0.1/36$.

No of grid points	*Order of convergence, p*					
N	$\|\mathbf{v}\|_1$	$\|\mathbf{v}\|_2$	$\|\mathbf{v}\|_\infty$	$\|\phi\|_1$	$\|\phi\|_2$	$\|\phi\|_\infty$
109	1.81	1.78	1.76	1.76	1.64	1.45
325	1.98	1.97	1.97	1.97	1.95	1.92
973	2.00	2.00	2.00	2.00	2.00	1.99

Table 1: Measured order of accuracy, p for the velocity field v and the volume fraction ϕ. $\varepsilon = 0.005$. Computations until $t = 4.0s$.

References

[1] Auzerais F.M., Jackson R.J., Russel W.B. *The resolution of shocks and the effect of compressible sediments in transient settling.* J. of Fluid Mechanics, 195:437-462 (1988)

[2] Bürger R., Wendland W.L., Concha F. *Model equations for gravitational sedimentation-consolidation processes* ZAMM, Z. Angew. Math. Mech. 80, 2:79-92 (2000)

[3] Dorobantu M. *One-Dimensional Consolidation Models.* Licentiate's thesis, Department of Numerical Analysis and Computer Science, Royal Institute of Technology, SWEDEN (1997)

[4] Gustavsson K., Oppelstrup J. *Numerical 2D models of consolidation of dense flocculated suspensions* J. of Engineering Mathematics, 41:189-201 (2001)

Finite Element Analysis of a Class of Viscoelastic Materials with Long Memory under Conditions of Friction

Pradeepa Nair* and Amiya K. Pani

Indian Institute of Technology, India

In this paper, we consider the finite element Galerkin approximations of a class of viscoelastic materials with a long memory under the effect of frictional conditions. The problem is first formulated in the form of a variational inequality and the frictional forces are included in the formulation in the form of a non differentiable functional. We then approximate the friction functional by a convex differentiable functional and transform the variational inequality formulation into a variational equality form. Subsequently, existence and uniqueness results are discussed using *a priori* bounds and compactness arguments. Discretizing in the spatial direction, we consider the semidiscrete scheme and the related error estimates are derived in suitable norms. Finally, using time discretization, we establish the error estimates for the completely discrete schemes.

On global solvability for a dissipative dusty gas model

G. G. Doronin*

Universidade Federal da Paraíba, 58109-970, Campina Grande, Brazil

N. A. Larkin

Universidade Estadual de Maringá, 87020-900, Maringá, Brazil

This talk concerns the global existence, uniqueness and asymptotic behavior of regular solutions for a mathematical model of the two-phase flow of a dusty medium. One phase is the carrier field (a fluid or gas) and the other one consists of small solid particles.

Historically, interest in two-phase flows dates from the 1940s. One of the first mathematical works is, probably, Ref.[1]. The main feature of the corresponding PDE-system is that, in general, it possesses both real and complex characteristic values and therefore it is not hyperbolic. This circumstance makes the well-posedness of the initial/boundary-value problems doubtful and complicates the stability and convergence of numerical algorithms, [2].

A particular example of a two-phase medium is a gas or liquid with suspended dust particles, known as "dusty gas", [3]-[5]. Although the characteristics of the corresponding system of PDEs are real, it nonetheless fails to be hyperbolic. The Cauchy problem for this model does not possess solutions, even locally in time, within classes of functions with a finite number of derivatives [6]. Similar phenomena were discussed in [7].

To overcome these troubles, one uses either two-pressure models (which ensure hyperbolicity), [2, 8], or models that take dissipative mechanisms into account, [9]-[13]. Our attention is focused on the second approach.

If the viscosity of a carrier medium is considered, then local-in-time solvability of the Cauchy problem is proved [11]. A first step towards the global solvability is given in [12]. In that work the local concentration of particles has been replaced by its averaged constant concentration. However, results on the existence of global regular solutions for original viscous dusty gas model are lacking. This is not surprising, since nonlinear hyperbolic equations, such as the momentum and continuity equations for the dust particles, generally speaking are solvable only locally in time. On the other hand, it is well-known that the presence of a linear damping term in hyperbolic equations together with sufficiently small initial data yield, at times, the existence of strong and even classical solutions for all $t > 0$. This leads us to expect a global solvability for dusty gas models with appropriate dissipation in the carrier phase.

Here we propose to model the principal (carrier) phase by the Kuramoto-Sivashinsky (KS) equation which has the viscosity term of the fourth order and is widely used in the theory of viscous turbulent flows and in studies of propagation of flame fronts [14, 15]. The latter ones provide classical examples of dusty media.

Thus, we study the composite PDE-system consisting of the KS equation for the carrier phase and nonlinear first-order hyperbolic equations for the dust particles. The equations are coupled by a nonlinear phase interaction term which contains the implicit damping. In the one-dimencional case the model is:

$$u_t + uu_x + \mu u_{xx} + \nu u_{xxxx} + \alpha u = mK(v-u),$$

$$v_t + vv_x = K(u-v),$$

$$m_t + (mv)_x = 0.$$

Here u and v are velocities of the medium and solid particles respectively; m is the local concentration of particles; μ, ν and α are positive constant coefficients of viscosity and friction, and $K > 0$ is the constant coefficient of the phase interaction.

Our goal is to investigate the mixed and Cauchy problems for this system. We prove the existence, uniqueness and exponential decay of global strong solutions for sufficiently small initial data.

References

[1] Rakhmatulin, Kh.A., *The basic gas dynamics of interpenetrating motions of compressible media* (in Russian), Prikl. Mat. Mekh., 1956, *20*, 185-195.

[2] Stewart, H.B.; Wendroff, B., *Two-phase flow: models and methods*, J. Comput. Phys., 1984, *56*, 363-409.

[3] Sproull, W.T., *Viscosity of dusty gases*, Nature 1961, *190*, 976.

[4] Kazakevich, F.P.; Krapivin, A.M., *Investigations of heat transfer and aerodynamical resistance in tube assemblies when the flow of gas is dustladen* (in Russian), Izv. Vissh. Uchebn. Zavedenii, 1958, *Energetica 1*, 101.

[5] Kliegel, J.R.; Nickerson, G., *Flow of a mixture of gas and solid particles in an axisymmetric nozzle*, In *Detonation and two-phase flow*, Penner, S.S., Williams, F.A., Eds; New York, 1962.

[6] Doronin, G.G.; Larkin, N.A., *Cauchy Problems for Equations of Two-Phase Flow*, In *Differential Equation Theory*, Ed. A.M.Blokhin, New York, 1996.

[7] Lax, P.D., *On the Notion of Hyperbolicity*, Comm. Pure. Appl. Math., 1980, *XXXIII*, 395-397.

[8] Nigmatulin, R.I. *Dynamics of multiphase media* (in Russian), Nauka, Moscow, 1987.

[9] Saffman, P.G., *On the stability of laminar flow of a dusty gas*, J. Fluid Mech., 1962, *13* (1), 120-128.

[10] Crooke, P.S., *On growth properties of solutions of the Saffman dusty gas model*, Z. Angew. Math. Phys., 1972, *1* (23), 182-200.

[11] Doronin, G.G., *Correctness of the Saffman model of a dust-laden gas with allowance for compressibility*, Differential Equations, 1995, *31* (6), 952-959.

[12] Larkin, N.A., *A model system of equations of the mechanics of heterogeneous media* (in Russian), Chisl. Metody Mekh. Sploshn. Sredy, 1978, *9* (7), 60-66.

[13] Doronin, G.G., *On solvability of the Cauchy problem for the dusty gas equations*, Comp. Appl. Math., 1999, *18* (2), 163-172.

[14] Kuramoto, Y.; Tsuzuki, T., *On the formation of dissipative structures in reaction-diffusion systems*, Prog. Theor. Phys., 1975, *54*, 687-699.

[15] Sivashinsky, G.I., *Nonlinear analysis of hydrodynamic instability in laminar flames*, Acta Astronautica, 1977, *4*, 1177-1206.

4.34 Thursday, Session 5 (afternoon): Numerical methods II

High Resolution Conjugate Filters for Hyperbolic Conservation Laws

Y. C. Zhou* and G. W. Wei

Department of Computational Science, National University of Singapore, Singapore

One of the most fascinating phenomena of hyperbolic systems is the presence of shock waves. Numerous numerical schemes have been developed for shock capturing since von Neumann and Richtmyer's genius conceiving of using artificial viscosity to eliminate spurious oscillations near a shock. Most of prevalent shock-capturing methods have inherited their idea of shock capturing by using additional viscosity. The incorporation of additional viscosity basically can be realized by one of two means, one is to explicitly add a diffusion term in original or discretized governing equations, and the other is to discretized the equation with an upwind type of biased stencils which will lead to a distinct dissipation term in the discretized equation [2]. Although the additional viscosity makes it possible to control the spurious oscillations near the discontinuity, it also degrades the formal numerical order and resolution of a scheme. To judiciously control the viscosity within an appropriate level is a nontrivial task, particularly in situations where a shock is interacting with other complex flow phenomena such as acoustic waves, vortices or turbulence eddies. The difficulty in handling these situations has stimulated the continuous interest in shock-capturing.
High-order schemes usually have higher resolutions with respect to the Fourier analysis than low-order ones. In the Fourier domain, high-order schemes give a wider region of correct wavenumber than low-order schemes. This observation initiates the work in optimizing the basic (compact) finite difference schemes with respect to an effective wavenumber range[1]. In the Fourier analysis, it is easy to see that beyond an effective wavenumber range, a numerical scheme will lost its accuracy. The Fourier spectrum of a shock is scattered over the whole Fourier domain. Therefore, the error in predicting the high frequency components will be accumulated and amplified during iterations and lead to spurious oscillations near the shock. As aforementioned, the suppression of these oscillations is generally achieved by introducing some dissipative terms in the numerical schemes. In this work, we discuss an alternative approach, the conjugate filter oscillation reduction (CFOR) scheme[3] for hyperbolic conservation laws. The use of nonlinear filters for shock-capturing was considered by Engquist et al[4].
The CFOR scheme has three distinct features. First, the scheme is based on a high order discrete singular convolution (DSC) algorithm [5], which provides a controllable accuracy for the spatial discretization in a smooth region. The accuracy of the DSC is very competitive with the Fourier pseudo-spectral method. Secondly, the conjugate high-pass and low-pass filters are constructed form a single generating function. Therefore, they have essentially the same support, regularity, smoothness and time-frequency localization. It is in this sense that they are *conjugated*. Finally, the effective frequency bandwidths of both high-pass and low-pass filters are independently adjustable. This makes it possible to design a low-pass filter which can conjugate with a high-pass filter on a wavenumber region as wider as possible, while most effectively reduce spurious oscillations.
In this work, we explore the performance of the CFOR scheme with a different DSC kernel, the Hermite kernel

$$\delta_{\Delta,\sigma}(x-x_k)=\frac{1}{\sigma}\exp\left(-\frac{(x-x_k)^2}{2\sigma^2}\right)\sum_{k=0}^{n/2}\left(-\frac{1}{4}\right)^k\frac{1}{\sqrt{2\pi}k!}H_{2k}\left(\frac{x-x_k}{\sqrt{2}\sigma}\right), \tag{1}$$

where $H_{2k}(x)$ is the usual Hermite polynomial and Δ is the grid spacing. Expression (1) is used as the low-pass filter and its two conjugated high-pass filters are generated by differentiation $\frac{d^q}{dx^q}\delta_{\Delta,\sigma}(x-x_k), \quad (q=1,2)$. The frequency response of the high-pass and low-pass filters constructed by using the Hermite kernel is plotted in Fig. (1). Numerical experiments are carried out in the rest of this paper with $n=88$ and $\frac{\sigma}{\Delta}=3.05$. Three examples are employed to access the accuracy, stability and resolution of the CFOR scheme with the Hermite kernel (CFOR-Hermite). Our numerical tests include a 1D advection equation, a 1D compressible Euler system and a 2D compressible Euler system.
EXAMPLE 1 *Advection of a sine-Gaussian wavepacket*
In this problem, a narrow Gaussian envelope modulated by a sine wave moves inside the computation domain [-1,1], governed by the linear wave equation $u_t+u_x=0$ with periodic boundary conditions. The sine-Gaussian wavepacket is defined as

$$u(x,t_0)=\sin[2\pi k(x-x_0)]e^{\frac{(x-x_0)^2}{2\sigma_0^2}}, \tag{2}$$

where $x_0=0$ is the location of the wave center at the initial time $t_0=0$ and $\sigma_0=\sqrt{2}/10$. The errors of the numerical results with respect to the exact solution is listed in Table 2. The time increment is chosen such that the overall error is dominated

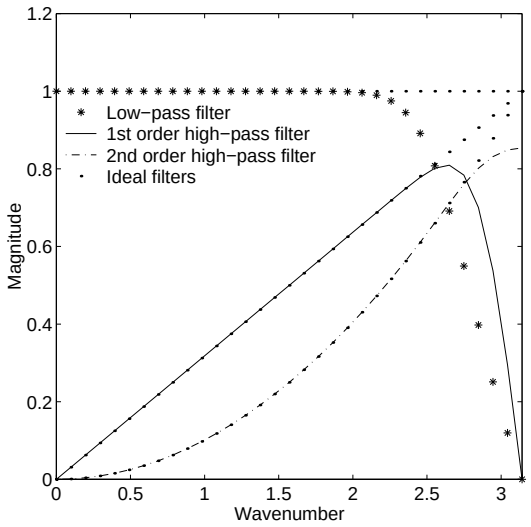

Figure 1: Frequency responses of the conjugate Hermite filers (in the unit of $1/\Delta$). The maximum amplitude of the filters is normalized to the unit.

Time	k(PPW)					
	5(20)	10(10)	15(6.7)	20(5)	25(4)	30(3.3)
2	1.17E-14	4.77E-14	4.23E-14	5.86E-12	2.21E-8	4.70E-5
4	2.11E-14	8.86E-14	8.23E-14	1.17E-11	4.43E-8	9.41E-5
6	2.46E-14	1.36E-13	1.11E-13	1.76E-11	6.64E-8	1.41E-4
8	3.19E-14	1.79E-13	1.46E-13	2.35E-11	8.86E-8	1.88E-4
10	4.01E-14	2.27E-13	1.73E-13	2.93E-11	1.11E-7	2.36E-4

Table 2: L_1 error for advancing the sine-Gaussian wavepacket ($\Delta t = 5 \times 10^{-6}, \Delta x = 0.01$.

by the CFOR-Hermite spatial differentiation. We compute the CFOR-Hermite results at a variety of k values. The ratio of grid points per wavelength (PPW) is calculated for each case. For a successful scheme, a smaller PPW indicates a higher numerical resolution. Extremely high accuracy is obtained for $k \leq 20$. For larger k values, numerical errors are limited by the differentiation errors. However, even at 3.3 PPW, the present errors remain very small.

EXAMPLE 2 *Free advection of a 2D isentropic vortex*

This example describes the free evolution of a 2D vortex described by the compressible Euler equations with periodic boundary conditions. For the detail definition of the problem please refer to [2]. The numerical errors and the formal order of the CFOR-Hermite scheme are tabulated and compared those of Garnier et al[2]. We also list the errors at $T = 10, 20, 50$ and 100 for the mesh of 80 $\times$ 80. In such a long time evolution, the CFOR-Hermite scheme is used to stabilize the nonlinear growth of errors. Obviously, the errors reflect the extremely small disparity between computed vortex and the idea vortex, which is supposed to be invariant during the time evolution. It can be seen that the CFOR-Hermite scheme is highly accurate and stable.

EXAMPLE 3 *Shock/entropy wave interaction*

Finally, we use a benchmark example[6] to demonstrate the shock-capturing ability of the CFOR-Hermite scheme with natural high frequency oscillations. In this problem, a small amplitude entropy wave is compressed by a moving shock. After the shock, the amplitude is amplified and the frequency is increased. Linear analysis provides quantitative results which are used to calibrate our numerical results. The problem is defined in a computation domain [0,5] and the initial condition for 1D compressible Euler system is

$$(\rho, u, p) = \begin{cases} (3.85714, & 2.629369, & 10.33333); & x \leq 0.5 \\ (e^{-\epsilon \sin(kx)}, & 0, & 1.0); & x > 0.5 \end{cases} . \tag{3}$$

The results are evaluated when the shock moves to $x = 4.5$ [6]. The entropy waves of two different wavenumbers(k=13 and k=65) are computed with the meshes of $N = 800$ and 1200, respectively. The corresponding PPW values for the generated waves are 20 and 6, respectively. Two solid lines wrapping the high frequency wave are the bounds from the linear analysis. It

N		CFOR	C4	ENO	MUSCL	WENO	ENO^A	WENO^A
40	error	2.37E-5	1.13E-3	1.28E-3	2.39E-3	9.39E-4	7.81E-4	6.11E-4
80	error	4.73E-9	5.78E-5	2.08E-4	5.99E-4	7.07E-5	6.68E-5	4.58E-5
	order	12.29	4.29	2.62	1.99	3.73	3.55	3.74
160	error	3.34E-10	3.79E-6	3.01E-5	1.26E-4	2.46E-6	7.84E-6	2.95E-6
	order	3.82	3.93	2.79	2.25	4.84	3.09	3.97
320	error	5.12E-11	2.41E-7	4.07E-6	2.26E-5	8.52E-8	6.82E-7	2.13E-7
	order	2.71	3.97	2.89	2.47	4.85	3.52	3.79

Table 3: L_2 error for the density at t=2; The CFL number is 0.5; C4: fourth-order accurate, conservative centered scheme; ENO: third-order; MUSCL: third-order; WENO: fifth-order; XXX^A denotes that the C4 scheme is used as the basic scheme with the XXX being a characteristic-based filter, while Harten's artificial compression method is used as a sensor to indicate the local numerical dissipation, see Ref. [2].

Time	2	10	50	100
L_1	4.73E-9	1.23E-8	4.58E-8	1.05E-7
L_2	1.41E-8	3.64E-8	1.41E-7	3.17E-7

Table 4: Errors for the density at different times (CFL=0.5, N=80).

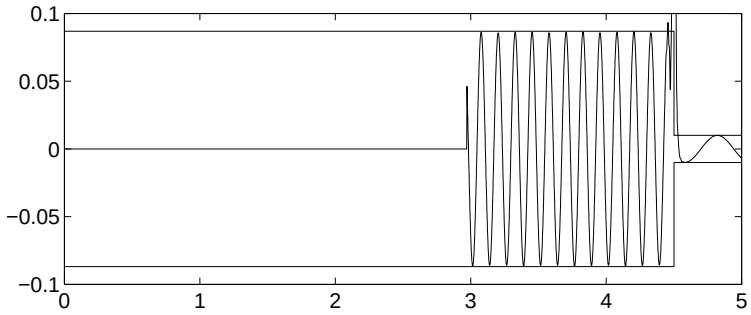

Figure 2: k=13, N=800, PPW=20

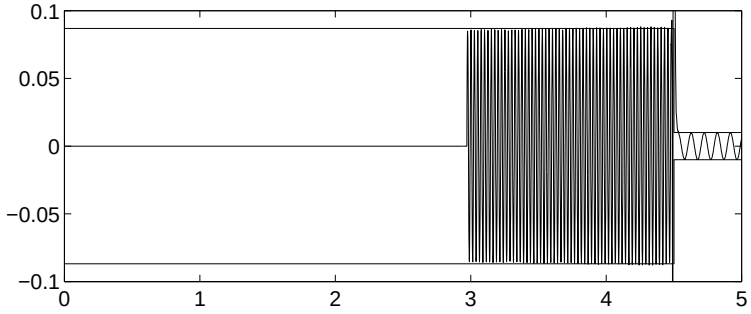

Figure 3: k=65, N=1200, PPW=6

is seen that the present results agree very well with the linear analysis. The high frequency waves at $k = 65$ are well resolved. It is very difficult for most existing low-order schemes to resolve such high frequency waves with such a small PPW ratio due to their intrinsic narrow effective wavenumber range and excessive dissipation.

References

[1] Sanjiva K. Lele, 'Compact Finite Difference Scheme with Spectral-like Resolution'. *J. Comput. Phys.*, **103**, 16-42, 1992.

[2] E. Garnier, P. Sagaut and M. Deville, 'A Class of Explicit ENO Filters with Application to Unsteady Flows', *J. Comput. Phys.*, **170**, 184-204, 2001.

[3] G. W. Wei and Yun Gu, 'Conjugated filter approach for solving Burgers' equation', *J. Comput. Appl. Math.*, revised; arXiv:math.SC/0009125, Sept. 13, 2000.

[4] B. Engquist, P. Lötstedt and B. Sjögreen, Nonlinear filters for efficient shock computation, *Math. Comput.*, **186** 509-537, 1989.

[5] G. W. Wei, 'Discrete Singular Convolution for the Solution for the Fokker-Planck Equations', *J. Chem. Phys.*, **110**, 8930-8942, 1999.

[6] Chi-Wang Shu, 'Essentially Non-Oscillatory and Weighted Essentially Non-Oscillatory Schemes for Hyperbolic Conservation Laws', ICASE TR-97-65, 1997.

A Deterministic Particle Method for Numerical Computations of Solitary Waves

Alina Chertock

University of California and LBNL, Berkeley, CA 94720

In recent years, particle methods have become one of the most useful and widespread tools for approximating solutions of partial differential equations in a variety of fields. In these methods, a solution of a given equation is represented by a collection of particles, located at points x_i and carrying masses w_i. At later times, the locations of the particles and/or their weights are allowed to change. The solution is then found by following the time evolution of the locations and of the weights of the particles according to a transport equation. Due to the Lagrangian nature of the method, small scales that might develop in the solution can be easily captured with a small number of particles. This property is what made particle methods so attractive in practice.

We present a new *dispersive-velocity* particle method for approximating solutions of linear and nonlinear dispersive equations [1]. This is the first time that particle methods are used for approximating this type of equations. Our method is based on the diffusion-velocity method, which was introduced by Degond and Mustieles [3] for approximating solutions of parabolic equations. In the *diffusion-velocity* method, one defines a convective field associated with the heat operator which then allows the particles to convect in a standard way [5, 6]. For example, the linear heat equation, $u_t - \nabla \cdot (S(x,t) \cdot \nabla u) = 0$, is rewritten as $u_t + \nabla \cdot (A(x,t)u) = 0$, where the velocity $A(x,t)$ is given by $-S(x,t) \cdot \nabla u(x,t)/u(x,t)$. Particles carrying fixed masses will then be convected with speed $A(x,t)$.

The new *dispersive-velocity* particle method is the first particle method to be proposed per se for approximating solutions of linear and nonlinear dispersive equations. Most importantly, this is the first attempt to use particles for directly simulating interaction between solitary waves. The main analytical result we provide is the short time existence and uniqueness of a solution to the resulting dispersion-velocity transport equation. The proof requires the initial data to have only one bounded derivative and provides the same regularity for the resulting solution.

We numerically test our new method for a variety of linear and nonlinear problems. Since we would like to demonstrate the advantages of the new techniques when compared with traditional finite-differences methods we focus our research on problems which develop non-smooth fronts and are therefore difficult to solve numerically. Among other examples are so-called $K(m,n)$ equations $u_t + (u^m)_x + (u^n)_{xxx} = 0$, $m > 0$, $1 < n \leq 3$, introduced by Rosenau and Hyman in [7]. The fundamental solutions of the $K(m,n)$ equation are compactly supported solitons, *compactons*. We consider the following nonlinear compacton equation $u_t + (u^2)_x + (u(u)_{xx})_x = 0$. This equation enjoys the richness of the features of nonlinear dispersive equations while, from the technical point of view, it is simpler to deal with. Since it is already written in an advective form, the velocity $a = u + u_{xx}$ depends linearly on u and its derivatives.

Due to the discontinuity in the derivatives on the fronts of compactons, standard numerical methods such as finite-differences and pseudo-spectral methods generate spurious oscillations on the fronts. Controlling these oscillations calls for a numerical filtering of the higher modes, which might result in the elimination of fine scales from the solution. Moreover, in cases where a positive solution should remain positive in time, the spurious numerical oscillations might cause the solution to change sign. In

this case, one can fall into an ill-posed region of the equation, and the numerical solution will cease to represent the solution of the equation at hand. We would like to offer here a different approach to address the complex numerical issues using particle method approximations.
We also apply the new dispersive-velocity method to nonlinear dispersive equations that when written in a convective form, do not have a linear dependence on the solution and its derivatives [2]. In this context, our model problem is the KdV equation introduced by Korteweg and de Vries in [4], $u_t + 3(u^2)_x + u_{xxx} = 0$. This equation which was developed for modeling shallow water waves, has been found relevant in other physical models such as, e.g., ion acoustic waves in a plasma and acoustic waves in an anharmonic crystal.
Numerical experiments show that the new particle method is capable of capturing the nonlinear regime of a compacton-compacton and a soliton-soliton interaction. We have also compared our particle method simulations with results obtained with a pseudo-spectral method. It is important to note that the results of the particle method do not suffer from spurious oscillations that are present in the spectral methods.
Areas of applications of the new dispersive-velocity method are not restricted to dispersive equations. In particular, we focus our attention on using the method for solving systems of hyperbolic conservation laws, including equations that describe multicomponent flows.
This is a joint work with D. Levy.

References

[1] Chertock A., Levy D., *Particle Methods for Dispersive Equations*, JCP, **171**, (2001), pp.708–730.

[2] A. Chertock, D. Levy, *Particle methods for the KdV equation*, Report LBNL-48963, Lawrence Berkeley National Laboratory, University of California Berkeley, October 2001, Journal of Scientific Computing, accepted.

[3] Degond P., Mustieles F.J., *A Deterministic Approximation of Diffusion Equations Using Particles*, SIAM J. Sci. Stat. Comp., **11** no. 2, (1990), pp.293–310.

[4] Korteweg D.J., de Vries G., *On the Change of Form of Long Waves Advancing in a Rectangular Canal and on a New Type of Long Stationary Waves*, Phil. Mag., **39**, (1895), pp.422–443.

[5] Lacombe G., *Analyse d'une équation de vitesse de diffusion*, preprint.

[6] Lacombe G., Mas-Gallic S., *Presentation and Analysis of a Diffusion-Velocity Method*, ESAIM: Proceedings, **7**, (1999), pp.225–233.

[7] Rosenau P., Hyman J.M., *Compactons: Solitons with Finite Wavelength*, Phys. Rev. Let., **70** no. 5, (1993), pp.564–567.

An Accurate Deterministic Projection Method for Stiff Detonation Waves

Alexander Kurganov

Tulane University, USA

Consider the reactive Euler equations that model the inviscid, compressible, reacting flow (without heat conduction). In the one-dimensional case, the equations take the form,

$$\vec{u}_t + \vec{f}(\vec{u})_x = \frac{1}{\varepsilon}\vec{S}(\vec{u}), \tag{1}$$

with $\vec{u} = (\rho, \rho u, E, \rho z)^T$, $\vec{f}(\vec{u}) = (\rho u, \rho u^2 + p, u(E+p), \rho u z)^T$, $\vec{S}(\vec{u}) = (0, 0, 0, -\rho z e^{-\tau_c/\tau})^T$. Here, $\rho, \rho u$ and E are the density, momentum and total energy, respectively. z is the fraction of unburnt fluid, $\vec{S}(\vec{u})/\varepsilon$ is a stiff reaction term with the small reaction time $0 < \varepsilon << 1$. The pressure for ideal gas is given by the equation of state (EOS), $p = (\gamma - 1)\left(E - \frac{1}{2}\rho u^2 - q_0 \rho z\right)$,

with $\gamma = 1.4$. Finally, the temperature is defined as $\tau = p/\rho$, and the parameters q_0 and τ_c stand for chemical heat release and ignition temperature.

In this model, the chemical reaction scales are typically orders of magnitude faster than the time scales of the corresponding hyperbolic system,

$$\vec{u}_t + \vec{f}(\vec{u})_x = 0. \tag{2}$$

This leads to problems of numerical stiffness – in order to compute an accurate approximate solution of (1), one has to use very small time steps, $\Delta t \sim \varepsilon$, which cannot be afforded in the most of practical applications. That is why we are interested in underresolved numerical methods, where $\Delta t >> \varepsilon$. Typically, such methods use the operator splitting, consisting of two steps:

1) Solving the homogeneous system by a high-resolution shock-capturing method,

2) Projection step for the stiff reaction term – chemically nonequilibrium data is projected into the equilibrium ones according to the ignition temperature value.

It was first observed by Colella, Majda and Roytburd [4], that such methods may lead to spurious, nonphysical shock waves, traveling with an artificial speed of one grid cell per time step. The incorrect speed is caused by the (deterministic) projection. This occurs because the numerically smeared nonequilibrium temperature, once above the given ignition temperature, triggers the chemical reaction too early, forcing the front to move.

Recently, Bao and Jin [2, 3] have proposed random projection methods for the reactive Euler equations. The key idea was to replace the ignition temperature, used in the projection step, with a uniformly distributed random variable, defined in a suitable interval. This approach guarantees the correct speed of detonation fronts, but reduces the overall accuracy of the scheme to the first one.

We propose an alternative, simple approach, which allows one both to correctly track the shock wave fronts and to achieve their high numerical resolution. The detonation waves are tracked by solving the purely hyperbolic system (2). At every time step, the computed values of z are used to update the EOS (without changing z itself) as follows. We use the deterministic projection method to obtain $\widetilde{z}_j^n = P(z_j^n), \widetilde{z}_j^n \in \{0, 1\}$, according to the value of ignition temperature τ_c (if $\tau > \tau_c$, then $\widetilde{z}_j^n = 0$, otherwise $\widetilde{z}_j^n = 1$). These new values $\{\widetilde{z}_j^n\}$ are then used in the EOS instead of $\{z_j^n\}$.

Put it differently, the last equation in (2) is used to "extract" the information needed for solving the first three equations of system (2). This approach resembles the level set model, used in the multifluid computations (see, e.g., [1]).

The performed numerical experiments demonstrate robustness and high accuracy of the proposed method. Its two-dimensional extension will be presented as well.

References

[1] R. Abgrall & S. Karni, *Computations of Compressible Multifluids*, Journal of Computational Physics **169** (2001), pp. 594–623.

[2] W. Bao & S. Jin, *The Random Projection Method for Hyperbolic Conservation Laws with Stiff Reaction Terms*, Journal of Computational Physics **163** (2000), pp. 216–248.

[3] W. Bao & S. Jin, *The Random Projection Method for Stiff Detonation Waves*, SIAM Journal on Scientific Computing **23** (2001), pp. 1000–1026.

[4] P. Colella, A. Majda & V. Roytburd, *Theoretical and Numerical Structure for Reacting Shock Waves*, SIAM Journal on Scientific and Statistical Computing **7** (1986), pp. 1059–1080.

[5] A. Kurganov & D. Levy, *Central-Upwind Schemes for the Saint-Venant System*, submitted to Mathematical Modelling and Numerical Analysis.

[6] A. Kurganov, S. Noelle & G. Petrova, *Semi-discrete central-upwind scheme for hyperbolic conservation laws and Hamilton-Jacobi equations*, SIAM Journal on Scientific Computing **23** (2001), pp.707–740.

Genuine Finite Volume Methods for Transport Equations with Constraints

M. Fey and M. Torrilhon*

Seminar for Applied Mathematics, ETH Zürich, Switzerland

Introduction

Many transport equations in physics and engineering come along with intrinsic constraints. Those constraints are expected to hold also in a numerical solution at least in a discrete manner. Nevertheless commonly available numerical methods do not care about intrinsic constraints of the equations. This paper will supply a general framework to derive numerical methods which

- control the constraint locally in every single timestep,
- use only one finite volume grid for the equation and the constraint,
- take upwind directions into account,
- perform a truly multidimensional update.

Some types of equations with constraints are given by the following table.

	transport equation:	constraint:
(A)	$\partial_t u + \operatorname{grad} F_A(u) = 0$	$\operatorname{curl} u = const$
(B)	$\partial_t u + \operatorname{curl} F_B(u) = 0$	$\operatorname{div} u = const$
(C)	$\partial_t u + \operatorname{div} F_C(u) = 0$	$\int u = const$

Examples of constrained transport equations like (A)-(C) arise in different areas of physics and engineering. The vorticity preserving of the balance law of momentum in fluid mechanics is of type (A). The Maxwell equations of electromagnetics form equations and constraints like in (B). Also the transport of the magnetic field in magnetohydrodynamics or the vorticity transport have the shape of (B). In general relativity the Einstein equations may be written in a form related to (B) with a divergence-type constraint. The last example (C) is an ordinary balance law with conservation of the variable u considered as constraint. The framework of this paper is also applicable to this case.

In [1] a model system with a constraint of type (A) and some numerical methods are investigated. In the literature one finds also many works which deal with divergence constraints (B) (e.g. [2]-[7]). In a local approach usually the divergence is conserved by using different grids for the equation and the constraint [3]/[5]. In [6] it could be shown that the staggered grid may be eliminated and thus the methods become more easy to implement. Nevertheless in the resulting schemes still remain some room for improvement. In [7] a locally constraint controlling method is developed via a FEM-type reconstruction. In this paper the staggered schemes of [5] and [6] as well as an advanced upwind method are derived together in a general framework. In [8] our upwind method together with the 'method of transport' have been successfully applied to the equations of magnetohydrodynamics.

The constrained transport equation may be written in the generic form

$$\text{transport: } \partial_t u + \mathcal{L}(u) = 0 \qquad \text{constraint: } \mathcal{C}(u) = const \tag{1}$$

where the constraint is intrinsic, i.e.

$$\mathcal{C}(\mathcal{L}(u)) \equiv 0. \tag{2}$$

On a finite volume grid $\mathcal{T} = \{K_i\}_{i=1,2,\dots}$ consisting of cells K_i with size bounded by h the linear contraint $\mathcal{C}$ is given by the discrete linear operator $\tilde{\mathcal{C}}$ up to a specific order

$$\mathcal{C}(u)|_K = \tilde{\mathcal{C}}_K \cdot u + O(h^n) \tag{3}$$

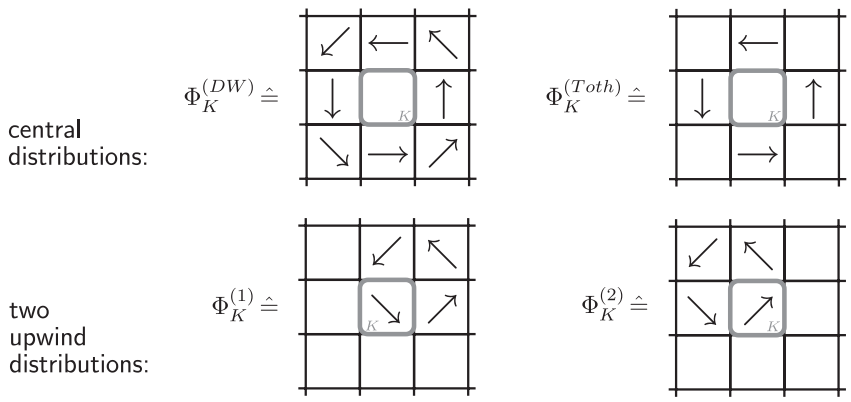

Figure 1: Divergence-free transport in two space dimensions. Examples of fieldline-fluxdistributions emerging from cell K. The updates by the fluxdistributions have to approximate closed curves to preserve the divergence locally in every timestep.

In this paper the central quantity is the so called *fluxdistribution* Φ_K, a grid function with $\operatorname{supp} \Phi_K = K \cup \mathcal{N}(K)$, where $\mathcal{N}(K)$ are the neighbouring cells of K. The value $\Phi_K(\hat{K})$ of the fluxdistribution gives the change of u at cell $\hat{K}$ caused by the cell K. Given a fluxdistribution then a numerical method is established by

$$u(t+\Delta t) = u(t) + \sum\nolimits_{\hat{K}} \Phi_{\hat{K}} + O(\Delta t^m) \tag{4}$$

where Δt is a timestep. To incorporate the constraint we require

$$\tilde{\mathcal{C}}_K \cdot \Phi_{\hat{K}} = 0 \quad \forall \hat{K}, K \tag{5}$$

to hold for the fluxdistribution. Thus it follows

$$\Rightarrow \quad \tilde{\mathcal{C}}_K \cdot u(t+\Delta t) = \tilde{\mathcal{C}}_K \cdot u(t) \tag{6}$$

i.e. the value of the discrete constraint is *preserved*. From Eqn (5) follows a linear system whose nontrivial solutions represent fluxdistributions that locally preserve the discrete constraint. The remaining parameters in the solutions of (5) are calculated by the consistency condition

$$\lim_{\Delta t, h \to 0} \frac{1}{\Delta t} \sum\nolimits_{\hat{K} \in \mathcal{N}(K)} \Phi_{\hat{K}}(K) \to \mathcal{L}(u)|_K \tag{7}$$

for the fluxdistribution with the transport equation in (1). The resulting method depends strongly on the used discretization $\tilde{\mathcal{C}}$ of the constraint and on the choice of the fluxdistribution out of the solutions of (5). In the following some fluxdistributions for a special case are discussed.

Divergence-free Advection

As a simple example for a constrained transport of type (B) we consider the divergence-free advection

$$\partial_t u + \operatorname{curl}(u \times v) = 0 \qquad \text{with} \quad \operatorname{div} u = const \tag{8}$$

Such an equation arises in magnetohydrodynamics as well as in the vorticity equation for fluid flows.
In two dimensions the variable u has the form $\left(u^{(x)}(x,y), u^{(y)}(x,y), 0\right)$ and the given advection velocity is $v = \left(v^{(x)}(x,y), v^{(y)}(x,y), 0\right)$. Additionally we have $\Phi_K(\hat{K}) \in \mathbb{R}^2$. For simplicity of presentation the grid is chosen as uniform and rectangular with $K \hat{=} (i,j)$.
In two dimensions the set of all discrete divergence operator with second order accuracy and 3×3 stencil is described by a 3-parametric family of operator matrices in (3)

$$C(\alpha,\beta,\gamma) = C_0 + \alpha C_1 + \beta C_2 + \gamma C_3 \qquad \alpha,\beta,\gamma \in \mathbb{R}. \tag{9}$$

Any choice for α, β and γ produces a second order accurate approximation of the divergence.